Electronic Supplementary Material (ESI) for Energy & Environmental Science.

Supplementary information

Assessing the Realism of Clean Energy Projections

Fatemeh Rostami[a], Piera Patrizio[b,c], Laureano Jimenez[a], Carlos Pozo[a,*], and Niall Mac Dowell[b,c]

[a]Departament d´Enginyeria Quimica, Universitat Rovira i Virgili, Tarragona 43007, Spain.
[b]Center for Environmental Policy, Imperial College London, London SW7 2AZ, UK.
[c]Center for Process Systems Engineering, Imperial College London, London SW7 2AZ, UK.

* Correspondence: carlos.pozo@urv.cat

Table of Contents

A: Technologies projected capacity

This section focuses on estimating the projected capacity of clean energy technologies (CETs) from 2020 to 2050 based on the Integrated Assessment Models (IAMs) for 1.5°C and 1.5°C with low overshoot temperature targets. The steps are as follows:

- **A.1: Technology selection:** We choose specific CETs along with their diverse types.
- **A.2: Exploring IAMs:** We use IAMs, particularly 8 different models including 25 scenarios in total, to estimate the capacity for each selected technology in terms of gigawatts (GW) for 1.5°C and 1.5°C with low overshoot targets.
- **A.3: Assigning capacity to each technology type:** IAMs typically provide capacity for an overall technology (e.g., photovoltaics) without specifying individual types (e.g., CdTe, CIGS, and CSi). To address this, we use market contribution data for diverse types of a technology to estimate their allocated capacity.
- **A.4: Presenting the capacity values:** We depict the annual and cumulative capacity for each selected technology and compare cumulative values with estimates from other sources such as International Energy Agency (IEA) and the International Renewable Energy Agency (IRENA). This comparative analysis helps realize the additional or reduced capacity needed to meet the temperature targets.

Each step will be elaborated on in the subsequent sections.

A.1: Technology selection

The list of technologies under consideration is presented in Table S1. While it appears in the manuscript, we have included it here for the sake of completeness.

Table S1: Considered CETs and technology types.

Technology category	Technology type	Technology full name and description
Battery	LFP	Lithium Ferro Phosphate
	NCA	Lithium Nickel Cobalt Aluminium
	NMC111	Lithium Nickel Manganese Cobalt (composition Ni/Mn/Co = 1/1/1)
	NMC622	Lithium Nickel Manganese Cobalt (composition Ni/Mn/Co = 6/2/2)
	NMC811	Lithium Nickel Manganese Cobalt (composition Ni/Mn/Co = 8/1/1)
	LiS	Lithium sulfide
	LiO	Lithium oxide
Concentrated solar power	FC	Fresnel Collector
	PT	Parabolic Trough
	ST	Solar Tower
Electrolyzers	Alkaline	Alkaline electrolyzer
	PEM	Proton Exchange Membrane electrolyzer
Photovoltaics	C-Si	Crystalline Silicon
	CIGS	Copper Indium Gallium Diselenide
	CdTe	Cadmium-Telluride
Wind turbines	AG	Asynchronous generator
	HTS-DD	High temperature superconductor - direct drive
	SG-E-DD	Synchronous generator - electrically excited - direct drive
	SG-PM-HS	Synchronous generator - permanent magnet - high speed gear
	SG-PM-MS	Synchronous generator - permanent magnet - middle speed gear
	SG-PM-DD	Synchronous generator - permanent magnet - direct drive

A.2: Exploring IAMs

Acknowledging that each IAM possesses unique scenario designs and technological resolutions, our analysis encompasses multiple IAMs to capture a broader spectrum of perspectives and account for variations in model assumptions. Specifically, we include eight distinct IAMs, encompassing a total of 25 scenarios which are presented in Table S2.[1]

The anticipated capacity for concentrated solar power systems (CSP), photovoltaics (PV), and wind turbines, as projected by IAMs, is generally based on their GW capacity. However, IAMs do not provide a direct projection for the capacity of batteries and electrolyzers in GW. Furthermore, IAMs provide cumulative capacity for CSP, PV, and wind, while our analysis requires annual capacity values. To address these discrepancies, additional calculations were performed, as explained next.

Table S2. Employed IAMs and scenarios under the "Below 1.5" and "1.5 low overshoot" targets.[1]

Model	Scenario	Technologies					
		Battery (Stationary)	Battery (EV)	CSP	Electrolyzer	PV	Wind
GCAM 4.2	SSP1-19				√	√	√
IMAGE 3.0.1	IMA15-AGInt			√	√	√	√
	IMA15-Def			√	√	√	√
	IMA15-Eff			√	√	√	√
	IMA15-LiStCh			√	√	√	√
	IMA15-Pop			√	√	√	√
	IMA15-TOT			√	√	√	√
	SSP1-19				√	√	√
MERGE-ETL 6.0	DAC15_50				√	√	√
MESSAGE-GLOBIOM 1.0	ADVANCE_2020_1.5C-2100			√		√	√
	EMF33_1.5C_cost100					√	√
	EMF33_1.5C_full					√	√
	SSP1-19				√	√	√
	SSP2-19				√	√	√
MESSAGEix-GLOBIOM 1.0	Low Energy Demand	√	√	√	√	√	√
POLES ADVANCE	ADVANCE_2020_1.5C-2100			√		√	√
REMIND-MAgPIE 1.7-3.0	PEP_1p5C_red_eff	√	√	√	√	√	√
	SMP_1p5C_Def	√	√	√	√	√	√
	SMP_1p5C_lifesty	√	√	√	√	√	√
	SMP_1p5C_regul	√	√	√	√	√	√
	SMP_2C_Sust	√	√	√	√	√	√
	SMP_1p5C_Sust*	√	√	√	√	√	√
	SMP_1p5C_early*	√	√	√	√	√	√
WITCH-GLOBIOM 4.4	CD-LINKS_NPi2020_1000			√		√	√
	CD-LINKS_NPi2020_400			√		√	√

* Scenarios belonging to the "Below 1.5" target.

Each model and scenario contribute to a broader understanding of potential futures and informs policy discussions. Awareness of the assumptions behind these scenarios, can provide insights into their effectiveness and feasibility.[1]

- GCAM 4.2, scenario SSP1-19 (Sustainability – Taking the Green Road):

This scenario envisions a gradual shift toward a sustainable path emphasizing inclusive development, improved global commons management, demographic transition, and reduced inequality. It focuses on human well-being, low material growth, and lower resource and energy intensity.

- **IMAGE Model**:

IMA15AGInt: Assumes high agricultural yields and intensified animal husbandry globally.

IMA15-Def: Implements climate policy through a uniform carbon tax in all regions and sectors from 2020 onward.

IMA15-Eff: Rapid application of best-available technologies for energy and material efficiency.

IMA15-LiStCh: Promotes a lifestyle change towards lower greenhouse gas (GHG) emissions, including dietary shifts and reduced use of CO_2-intensive transport.

IMA15-Pop: Based on SSP1 with low population growth projections.

IMA15-TOT: Combination of all the above options.

- **MESSAGE-GLOBIOM 1.0 Model:**

ADVANCE_2020_1.5C-2100: Strengthened ambition post-2020 to align with a long-term target of limiting warming to 1.5°C by 2100.

EMF33_1.5C_cost100 and EMF33_1.5C_full: Consider bioenergy technologies, such as Bio Energy with Carbon Capture and Storage (BECCS), Cellulosic fuels and Hydrogen.

SSP1-19: Choosing the Green Pathway (Minimal challenges to mitigation and adaptation) the global trajectory gradually veers towards sustainability, with a pervasive shift emphasizing inclusive development within perceived environmental limits. Progress in managing shared resources steadily enhances, while investments in education and healthcare accelerate demographic shifts. Economic priorities broaden to prioritize human well-being over mere growth. A growing commitment to development goals leads to decreased inequality both among and within nations. Consumption patterns favour minimal material growth and reduced resource and energy usage.

SSP2-19: In a Middle-of-the-road scenario (with moderate challenges to mitigation and adaptation), global trends in social, economic, and technological spheres remain relatively stable, aligning closely with historical patterns. Development and income growth vary across nations, with some countries achieving notable progress while others struggle to meet expectations. Efforts by global and national institutions to address sustainable development goals are ongoing but slow-moving. While environmental degradation persists, there are some signs of improvement, and overall, there's a gradual decline in resource and energy consumption. Global population growth maintains a moderate pace, reaching a plateau in the latter half of the century. Income inequality persists or improves at a sluggish rate, and challenges in reducing vulnerability to societal and environmental shifts persist.

- **MESSAGEix-GLOBIOM 1.0, scenario LowEnergyDemand**:

Limits global mean temperature increase to 1.5°C and achieves remarkable co-benefits for other sustainable development goals.

- REMIND-MAgPIE 1.7-3.0:

PEP_1p5C_red_eff: Scenario with a carbon budget of 400 Gt CO_2 from 2011-2100, reduced availability of carbon dioxide removal (CDR), and comprehensive carbon pricing.

SMP_1p5C_Def, SMP_1p5C_Sust, SMP_1p5C_early, SMP_1p5C_lifesty, SMP_1p5C_regul: Various scenarios with a 400 Gt CO_2 budget from 2011-2100, each emphasizing different policy approaches (default carbon pricing, sustainability policies, early action, lifestyle changes, regulation policies).

SMP_2C_Sust, SMP_2C_early: Scenarios with a 1000 Gt CO_2 budget from 2011-2100, focusing on sustainability and early action policies to limit warming to 2°C.

- WITCH-GLOBIOM 4.4:

CD-LINKS_NPi2020_1000, CD-LINKS_NPi2020_400: Transition scenarios from a New Product Introduction (NPi) scenario until 2020 to globally cost-effective carbon budget implementation for the period 2011-2100 (1000 Gt CO_2 for 2°C limit, 400 Gt CO_2 for 1.5°C limit).

A.2.1: Photovoltaics, concentrated solar power systems, and wind turbines

We extracted cumulative PV capacity data from 8 IAMs, including 25 scenarios, covering years 2005 to 2050 in five-year intervals (e.g., 2020, 2025, 2030, ...). The process to estimate the capacity added annually involved several steps:

- We created a plot of cumulative capacity against years and extracted the cumulative capacity for the remaining years (e.g., 2021, 2022, ...), since neither linear nor nonlinear regression proved to be a suitable fit.
- By calculating the capacity difference between consecutive years, we determined the capacity added annually.
- We estimated the Replaced Capacities (RC) resulting from the retirement of Previously Installed Capacities (PIC) for each year (n), assuming a 30-year lifespan for a typical PV panel, and using Eq. S1. Note that, in this analysis, we are investigating the period from 2020 to 2050. However, to estimate the required replacements, we extracted data from as early as 2005, which is the first year that IAMs have some capacity projections.

$$RC_{(n\ +\ lifespan)} = PIC_n \qquad \forall n \tag{S1}$$

- The total annual added capacity was then derived by summing the estimated annual capacity values from step two and the replaced capacities from step three.

We followed the same approach for concentrated solar power systems and wind turbines, considering a lifespan of 30 years.

While most IAM scenarios provide capacity projections for these technologies in GW, four of them - DAC15_50 from MERGE-ETL 6.0 model, EMF33_1.5C_cost100 and EMF33_1.5C_full from MESSAGE-GLOBIOM 1.0 model, and LowEnergyDemand from MESSAGEix-GLOBIOM 1.0 model - offer projections in EJ/yr. Therefore, for these scenarios, we initially divide the provided projections by the energy delivered annually from each of these technologies. Details on estimating the delivered energy for these technologies are provided in section D.1 (Eq. S27).

A.2.2: Batteries used for stationery and mobility applications

We distinguish between batteries used for stationery and mobility applications. For the former, we extracted Annual Investment (AINV) data for electricity storage between 2015 and 2050 from MESSAGEix-GLOBIOM 1.0 and REMIND-MAgPIE 1.7-3.0 models including 8 scenarios (see Table S2). These data are expressed in billions of US$2010 per year and provided for five-year intervals (e.g., 2020, 2025, 2030, …). Values for the remaining years were estimated using linear regression. Since batteries are just one alternative among other energy storage options, these values are multiplied by $Share^{BAT}$, providing the share of batteries in electricity storage [%] [2,3]. Then, we converted the resulting values to current € (2023), considering appropriate currency conversion (Con, [€/USD] [4]), and, subsequently, translated them to energy storage capacity using the price of a typical battery ($PRICE^{BAT}$, [€/Wh]). Finally, we transform these values into power capacity using the ratio between the power density ($PODENS$, [W/kg]) and the energy density ($ENDENS$, [Wh/kg]). The overall calculation used to obtain the capacity installed annually based on each IAMs scenario for batteries in year *n* ($CC^{BATSTO}_{n,s}$, [W]) is given by Eq. S2.

$$CC^{BATSTO}_{n,s} = AINV^{STO}_{n,s} \cdot Share^{BAT} \cdot Con \cdot \frac{1}{PRICE^{BAT}} \cdot \frac{PODENS}{ENDENS} \qquad \forall n = 2020, \ldots, 2050,\ s \tag{S2}$$

Values for battery price (e.g., 200 euros/kWh), power density (e.g., 750 W/kg), and energy density (e.g., 250 Wh/kg) are sourced from the literature [2,3]. It is important to highlight that power and energy density exhibit considerable variability. For instance, power density varies within the range of 50-2000 W/kg, while energy density changes from 150 to 350 Wh/kg[3]. For our calculations, we opted for 750 W/kg for power density and 250 Wh/kg for energy density, aligning with the characteristics of batteries used in power applications and electric vehicles. Importantly, as will be discussed in section B.1, selected values do not impact the estimated demand for materials. Still, accounting for these ranges allows to assess uncertainties in installed capacities. These are reported as error bars in Figures S1 and S2, where we compare the power capacity across different technologies.

Replaced capacities for batteries were calculated assuming a 15-year lifespan[5] (Eq.S1). Hence, the total capacity added is determined by adding the replaced capacities to the newly installed annual capacities[6]. Note that in this case data are available since 2015.

In addition to its primary role in electricity storage, batteries are anticipated to play a crucial role in electric mobility. As outlined by the European Technology and Innovation Platform on Batteries (2020)[7], there is a notable shift in the ratio of battery utilization for electric mobility compared to its application in energy storage ($\frac{BAT^{EV}}{BAT^{STO}}$ in Eq. S3). This ratio is projected to transition from approximately 23 in 2020 to 7.6 in 2025. Utilizing these varying ratios over time, and the capacity of batteries for energy storage determined previously, we calculated the capacity of batteries required for electric mobility ($CC^{BATEV}_{n,s}$) up to 2025 (Eq. S3).

$$CC^{BATEV}_{n,s} = CC^{BATSTO}_{n,s} \cdot \frac{BAT^{EV}}{BAT^{STO}} \qquad \forall n \leq 2025,\ s \tag{S3}$$

Based on the global electric vehicle outlook[8], the number of electric vehicles (EV) on the road was approximately 10 million in 2020. According to the Energy Technology Perspectives report, the projected manufacturing output for EV is 60 million units by 2030 and increases to 90 million by 2050[9]. These estimations align with the 1.5°C target.

Having the $CC^{BATEV}_{n,s}$ for 2020 from Eq.S3, as well as the Number of Electric Vehicle (NEV) in that year, we assumed a proportional ratio to estimate the capacity of batteries used in EV for 2030 and 2050 (Eq. S4-S5). Then, we employed a linear regression to estimate the capacity for intermediate years. Subsequently, we calculated the required replacements using Eq. S1, and added them to the annual capacities of new batteries to determine the final capacity added each year.

$$CC^{BATEV}_{2030,s} = CC^{BATEV}_{2020,s} \cdot \frac{NEV_{2030}}{NEV_{2020}} \qquad s \tag{S4}$$

$$CC^{BATEV}_{2050,s} = CC^{BATEV}_{2030,s} \cdot \frac{NEV_{2050}}{NEV_{2030}} \qquad s \tag{S5}$$

Acknowledging that these ratios may not necessarily yield a capacity value in alignment with the 1.5°C target, we employ them due to the absence of better data.

A.2.3: Electrolyzers

Under the secondary energy category, IAMs provide data on Annual Production (APROD) of hydrogen through electrolyzers between 2020 and 2050, with measurements given in [EJ/year] in five-year intervals, for each of the scenarios. Then, the capacity of the electrolyzers in year *n* and based on IAMs scenario s ($CC_{n,s}$, [W]) is determined using Eq. S6.

$$CC^{ELCTZ}_{n,s} = APROD^{H_2}_{n,s} \cdot \frac{1}{LHV^{H_2}} \cdot \frac{1}{ENGEN^{ELCTZ}} \cdot \frac{1yr}{365d} \qquad \forall n, s \tag{S6}$$

Here, $CC^{ELCTZ}_{n,s}$ is the capacity installed for electrolyzers in year *n* according to IAMs scenario s [GW] and LHV^{H_2} is the lower heating value of hydrogen [EJ/kg H_2]. Then, $ENGEN^{ELCTZ}$ is the hydrogen generation capacity of a typical electrolyzer [kg H_2/day·GW]. We acknowledge this value changes in a range for different types of the electrolyzers, so we considered it equal to 400 kg H_2/day·MW, which is a valid values for both, alkaline and PEM electrolyzers[10].

In all IAM scenarios, electrolyzer development starts mainly after 2030 with very minor values, and given its lifespan of more than 10 years, the replaced capacity before 2050 is negligible. Therefore, Eq.S6 directly provides the total capacity added annually.

A.3: Assigning capacity to each technology type

IAMs provide capacity projection for each technology but they do not distribute it among different technology types owing to a low technological resolution. Therefore, we employed the potential market share evolution of different technology types, as reported by the German Aerospace Centre[11], to allocate the total capacity projected for each technology to their respective types. Two different

market contribution scenarios are available in the report, one based on a "continued market trend" and another based on a "technological change market trend" for technologies deployment and diffusion. The former trend considers a smooth evolution of technologies, while the later one assumes that sudden technological changes might occur. Eq. S7 provides the details of the calculations, while Tables S3-S4 present the market contribution values for each technology (T) and its respected types (t)[11].

$$CCI_{t,n,s,k}^{T} = CC_{n,s}^{T} \cdot MC_{t,n,k} \qquad \forall n,k,\ t \in TT_T,\ s,\ T = \{BAT, CSP, ELECTZ, PV, WIND\} \tag{S7}$$

Here, $CCI_{t,n,s,k}^{T}$ is the capacity installed for individual type *t* of technology category *T* in year *n* according to IAMs scenario s and market trend *k* [GW], $CC_{n,s}^{T}$ is the capacity installed for technology category *T* in year *n* and according to IAMs scenario s [GW], and $MC_{t,n,k}$ is the market contribution of technology type *t* in year *n* according to market trend *k* [%]. The relationship between technology types *t* (e.g., SG-E-DD wind turbine) and technology categories *T* (e.g., wind turbines) is given by set TT_T, providing the technologies of type *t* that belong to category *T*.

Table S3: Market contribution of different technology types based on continued market[11].

Technology	Type	2020	2030	2040	2050
Battery (EV)	LFP	11	5	3	0
	NCA	13	8	13	13
	NMC111	20	0	0	0
	NMC622	50	32	20	15
	NMC811	6	55	64	72
Battery (Stationary)	LFP	39.8	39.8	39.7	39.7
	NCA	0	0	0	0
	NMC111	23.9	0	0	0
	NMC622	13.3	16.7	12.5	6.63
	NMC811	3.3	33.6	37.9	43.8
	Non lithium types	19.7	9.9	9.9	9.9
Concentrated solar power	FC	5	5	5	5
	PT	90	90	90	90
	ST	5	5	5	5
Electrolyzer	Alkaline	50	42	40	35
	PEM	50	58	60	65
Photovoltaic	C-Si	94	94	94	94
	CIGS	1	1	1	1
	CdTe	5	5	5	5
Wind turbine	AG	15	18	16	14
	SG-E-DD	57	50	50	50
	SG-PM-HS	28	30	31	31
	SG-PM-MS	0	2	3	5

Table S4: Market contribution of different technology types based on technological change trends[11].

Technology	Types	2020	2030	2040	2050
Battery (EV)	LFP	9.8	4.8	0	0
	NCA	14.7	10.1	5.6	0
	NMC111	25.5	0	0	0
	NMC622	44.5	27.8	10.9	0
	NMC811	5.5	47.9	32.7	0
	LiS	0	9.4	49.4	91.4
	LiO	0	0	1.4	8.6
Battery (Stationary)	LFP	39.1	22.3	20.3	19.9
	NCA	0	0	0	0
	NMC111	23.9	0	0	0
	NMC622	13.2	8.14	4.9	2.09
	NMC811	3.2	16.6	14.7	15.41
	Non lithium types	20.6	53	60.1	62.6
Concentrated solar power	FC	5	7	12	15
	PT	90	75	60	45
	ST	5	18	28	40
Electrolyzer	Alkaline	50	25	15	0
	HT SOEL (Yttrium)	0	3	12	25
	PEM	50	72	73	75
Photovoltaic	C-Si	96	83	73	63
	CIGS	1	5	9	12
	CdTe	3	12	18	25
Wind turbine	AG	12	7	3	1
	SG-E-DD	28	15	7	2
	SG-PM-HS	50	50	45	50
	SG-PM-MS	0	8	8	10
	HTS-DD	0	0	0	12
	SG-PM-DD	10	20	37	25

A.4: Presenting the capacity values

Figures S1 and S2, respectively, depict the anticipated annual and cumulative capacity of CETs until 2050. Note that since we use the annual capacities of CETs in our calculations, we provide their median values obtained from 25 scenarios. In addition, we compare our estimates with data from reports from the International Energy Agency (IEA)[7,12–17], the International Renewable Energy Agency (IRENA) [17], or any other source where projections are available. As depicted in Figure S2, the demand for batteries is predominantly influenced by their usage in electric vehicles. Furthermore, our estimated ranges based on IAMs projections align with the data reported from other sources.

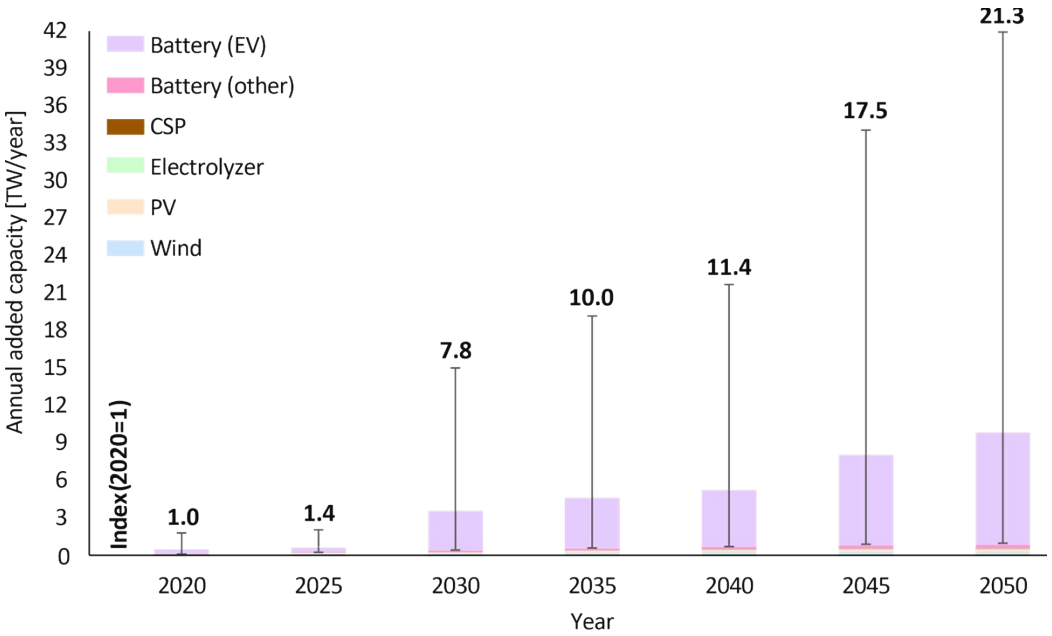

Fig.S1 Projections for the aggregated capacity of clean energy technologies added annually based on IAMs scenarios (Table S2). The numbers on top of the bars present the ratio of capacity added in each year over the capacity added in 2020. The error bars present the variations in the capacity added for batteries, depending on the battery characteristics, as discussed in section A.2.2.

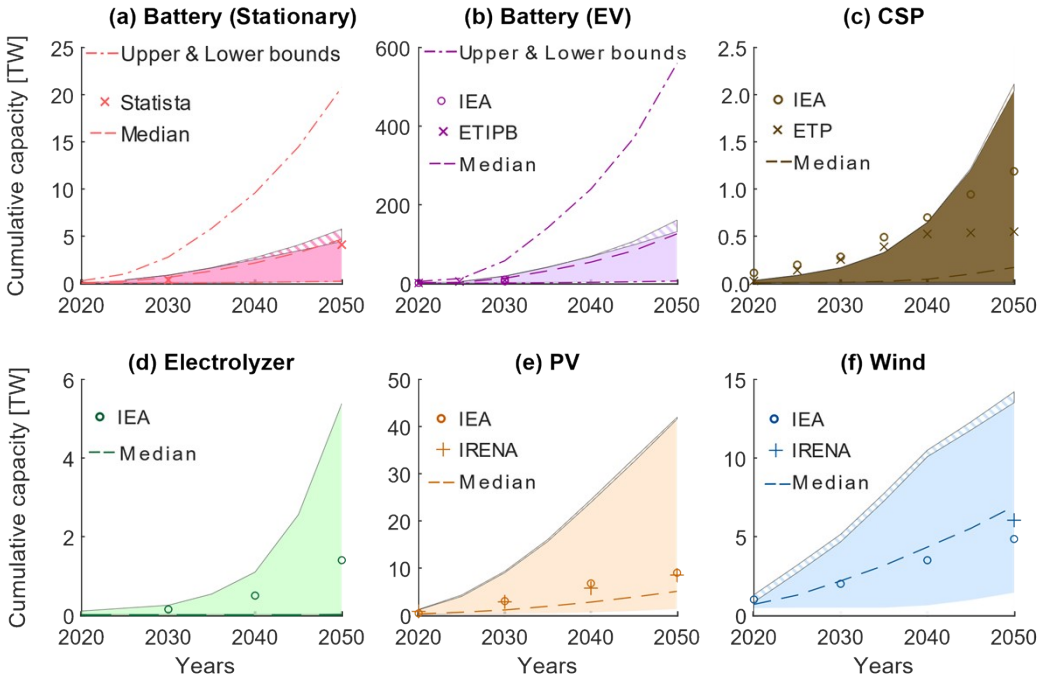

Fig.S2 Cumulative projected capacity of clean energy technologies based on IAMs (Table S2). For each technology, the projected capacity in 2020 is used as a base to estimate the ratio of projected capacity in 2050 over it, except for the electrolyzers, since their development starts mainly after 2030. In addition, the replaced capacity of each technology is presented in its panel by a dashed area. Markers in each panel represent data from additional sources used for comparison: circles show IEA projections,[14,18,19] plus signs denote IRENA data,[17] and cross signs correspond either to data from the European Technology and Innovation Platform for Battery (ETIPB),[7] from Statista (for stationary batteries projections),[13] or from the Energy Technology Perspectives (ETP) (for CSP).[12] Dashed lines present the median of projections. Notably, long dash dot lines present the upper bound and lower bound capacity for batteries (more on this can be seen in section A.2.2).

B: Materials demand estimation

This section is dedicated to estimating materials demand associated with the projected capacity of CETs from 2020 to 2050, as per IAMs and for selected temperature targets. The outlined steps are as follows:

- **B.1: Material intensities:** We conducted an extensive literature review to compile current intensity values (i.e., ton/GW capacity) for 36 different materials across various technology types. We also included the effect of learning curves to estimate a decrease in material intensity values over time.
- **B.2: Resulting classifications:** We derived material demand estimates for four distinct classes. Two market contribution scenarios to estimate allocated capacity for technology types (Continued and Technological change, section A.3), and two material intensity scenarios (Base and Learning). These are combined by 25 IAM scenarios (Table S2).
- **B.3: Calculation of material demands:** We multiplied the capacity allocated to each technology type by its respective material intensity values to derive the material demands. Specifically, we estimated material demand values for 25 IAM scenarios, providing detailed discussions.
- **B.4: Current production rate of materials, their reserve capacities, and recycling rate:** We provided a scale to the demand values estimated by comparing them with their current production rates, illustrating how demand will evolve over time.
- **B.5: Exploring the possibilities of by-products:** For materials generated as byproducts of others, we estimated their production by considering their relative concentration in the ores.
- **B.6: Estimated material demands:** We compared the estimated demand for materials over time with (i) their current production rate, and (ii) their current (i.e., 2020 due to data limitations) demand. Results for materials whose ratios are greater than one in both cases are discussed in the manuscript, while, in this section, we focus on the remaining materials. In addition, median values for material demands across scenarios in selected years are also presented. Results are compared with those from similar studies for validation.
- **B.7: Links between problematic materials and technology types:** We explored the relationship between problematic materials and the technology types expected to dominate the 2050 market.
- **B.8: Demand-to-reserves comparison:** Additionally, we provide an analysis of demand-to-reserves capacity ratios for problematic materials where this ratio approaches or exceeds one.

B.1: Material intensities

In this step, material intensity values for each technology type are collected. Technology learning curves are then used to estimate the impact of technology evolution. Table S5 provides a list of the materials considered, while a summary of material intensity values is presented in Tables S6-S8. Note that, for the case of PV and wind turbines, material intensity estimations consider the cabling requirements to connect the PV panels or the wind turbines to the grid[20]. Where more than a single value was available, we used the average of reported values. Additionally, material intensity values for some materials change over time due to the effects of technology learning curves, specifically for PV panels and wind turbines. However, for the types of batteries and electrolyzers included in our assessment, no significant changes are reported in their material intensities[11,20].

The values for aluminium, cadmium, concrete, copper, gallium, glass, indium, nickel, plastic, selenium, silicon, silver, steel, and tellurium used in PV panels, and Dy, Mn, Nd, Ni, and V used in wind turbines,

are updated for the next decades using the learning curves of the technologies as reported in Tables S7 and S8 [11,20]**.** Apart from these, the intensity of the iridium used in PEM electrolyzers changes from 0.88 ton/GW in 2020 to 0.20 ton/GW in 2030, 0.05 ton/GW in 2040 and stays constant until 2050. For platinum used in the same technology, the material intensity changes from 0.25 in 2020 to 0.07 in 2030, 0.04 in 2040 and stays constant until 2050 [11]. Similarly, the lithium used in LFP batteries drops from 43 ton/GW in 2020 to 40 ton/GW in 2050, while nickel intensity in NMC622 batteries changes from 197 ton/GW in 2020 to 141.5 ton/GW in 2050.

It is essential to note that material intensities for batteries is commonly expressed in ton/GWh in the literature. To convert these values to ton/GW, we multiply them by the energy density of batteries (e.g., 250 Wh/kg) and then divide it by their corresponding power density (i.e., 750 W/kg) [3]. It is worth emphasizing that, for estimating the capacity of batteries in GW, we multiplied the available data by power density and then divided the result by the corresponding energy density, as detailed in section A.2.2. Therefore, the final multiplication of capacity time intensity cancels out the power and energy density values. Ultimately, the material demand value, presented in tons, remains independent of these values.

In addition to the values provided in Table S6, we use the following values for CSP technologies: FC require 2045 [ton Mn/GW], 471 [ton Ni/GW], 31 [ton Ag/GW] and 2 [ton V/GW]; PT need 2047 [ton Mn/GW], 471 [ton Ni/GW], 25 [ton Ag/GW] and 1.9 [ton V/GW]; and ST demand 5600 [ton Mn/GW], 1785 [ton Ni/GW], 36 [ton Ag/GW] and 1.7 [ton V/GW].[11,20]

Table S5: List of the materials considered and their symbols.

Materials	Symbols	Materials	Symbols	Materials	Symbols	Materials	Symbols
Activated carbon	C	Gallium*	Ga	Manganese	Mn	Silica[a]	Sil.
Aluminium	Al	Glass[a]	Gla.	Molybdenum	Mo	Silicon	Si
Cadmium	Cd	Glass/Carbon composites/fiberglass[a]	GCC	Neodymium*[R]	Nd	Silver	Ag
Cement[a]	Cem.	Gold	Au	Nickel	Ni	Steel[a]	Ste.
Chromium	Cr	Graphite[a,] *	Gra.	Plastic[a]	Pla.	Tellurium	Te
Cobalt*	Co	Indium*	In	Platinum*[P]	Pt	Terbium*[R]	Tb
Concrete[a]	Con.	Iridium*[P]	Ir	Praseodymium*[R]	Pr	Titanium*	Ti
Copper	Cu	Iron	Fe	Resin PPS[b] - Glass fiber[a]	Res.	Vanadium*	V
Dysprosium*[R]	Dy	Lithium*	Li	Selenium	Se	Zinc	Zn

*: Critical material, *[R]: Critical and rare earth element (REE), *[P]: Critical and platinum group metal (PGM) [21].

[a]The presented symbol is not a standard symbol assigned to this material. It is defined by the author for the sake of simplicity in later referring.

[b]PPS: Polyphenylene Sulfide.

Table S6: Material intensities for CETs, except for CSP[a,b,c].

Technologies	Battery							Electrolyzer		PV			Wind				
Materials	LFP	NCA	NMC 111	NMC 622	NMC 811	LiS	LiO	Alkaline	PEM	CSi	CIGS	CdTe	AG	HTS-DD[d] SG-E-DD[d]	SG-PM-HS	SG-PM-MS	SG-PM-DD
Ag										18							
Al	353	539	451	409	366	353	353	75	65	7,500	7,500	7,500	4,990	700	1,600	1,600	500
Au									0.29								
C									13								
Cd											1	47					
Cem.[a]										7.7	7.7	7.7	55.3	48.5	54.3	54.3	32.0
Co	0	190	178	67	47	0	120										
Con.[a]										60.7	60.7	60.7	420	369	413	413	243
Cr														525	580	580	525
Cu	46	55	62	59	56	46	46	333	11	4,600	4,600	4,600	1,764	5,000	950	950	3,000
Dy														6	4.3	5	17
Fe[a]														20.1	20.8	20.8	20.1
Ga											4						
GCC[a]													7.7	8.1	8.1	8.1	8.1
Gla.[a]										46.4	46.4	46.4					
Gra.	274	352	325	340	354	274	274	72									
In											18	8					
Ir									0.88								
Li	43	60	50	57	57	120	53										
Mn		129	175	63	54	0	105						780	790	550	500	600
Mo														109	119	119	109
Nd														28	35	42	155
Ni	23	190	181	197	375	0	193	3167		2			410	340	420	442	410
Pla.	24	30	30	29	28	24	24	130		8,600	8,600	8,600	7,817	7,817	7,817	7,817	7,817
Pr														9	4	4	35
Pt									0.25								
Res.									136								
Se											39						
Si										4,000							
Sil.	4	7	7	7	7	6	6										
Ste.	11	13	14	14	14	11	11		1,928	67,900	67,900	67,900	124,654	66,000	107,000	107,000	119500
Tb														1	1	1	7
Te												51					
Ti									34								
V															90	90	90
Zn[a]													5,500	5,500	5,500	5,500	5500
Ref.	11,22,23							11,23,24		6,11,20,22			6,11,20,22,25,26				

[a]Values are in [ton/GW capacity], except for cem., con., gla., GCC, Fe, and Zn which are in [ton/MW capacity].
[b]Materials complete name is presented in Table S5.
[c]Values for CSP technology are provided in text before Table S5.
[d]Values for SG-E-DD wind turbines are also used for HTS-DD as this is the most similar technology[20].

Table S7: Change in material intensities driven by learning curves for PV panels [ton/GW capacity] [11,20].

Year	2020			2030			2040			2050		
Materials	C-Si	CIGS	CdTe	C-Si	CIGS	CdTe	CIGS	C-Si	CdTe	C-Si	CIGS	CdTe
Aluminium	7,500	7,500	7,500	7,200	7,200	7,200	7,000	7,000	7,000	6,800	6,800	6,800
Cadmium	0	1	46.5	0	1	42	0	1	23	0	1	21
Concrete	60,700	60,700	60,700	58,400	58,400	58,400	56,500	56,500	56,500	54,600	54,600	54,600
Copper	4,600	4,600	4,600	4,500	4,500	4,500	4,350	4,350	4,350	4,200	4,200	4,200
Gallium*	0	4.3	0	0	2.5	0	0	2	0	0	1.5	0
Glass	46,400	46,400	46,400	44,700	44,700	44,700	43,050	43,050	43,050	41,800	41,800	41,800
Indium*	0	17.7	8	0	15	4	0	11	1	0	9	0
Nickel	2	0	0	2	0	0	2	0	0	2	0	0
Plastic	8,600	8,600	8,600	8,300	8,300	8,300	8,000	8,000	8,000	7,700	7,700	7,700
Selenium	0	38.5	0	0	29	0	0	16	0	0	12	0
Silicon	4,000	0	0	2,750	0	0	2,325	0	0	2,000	0	0
Silver	18	0	0	10	0	0	4	0	0	3	0	0
Steel	67,900	67,900	67,900	67,900	67,900	67,900	63,150	63,150	63,150	61,100	61,100	61,100
Tellurium	0	0	50.7	0	0	34.6	0	0	25.3	0	0	22.9

Table S8: Change in material intensities driven by learning curves for wind turbines [ton/GW capacity] [11,20].

Year	2020					2030					2040					2050				
Materials	AG	SG-E-DD[a,b]	SG-PM-HS	SG-PM-MS	SG-PM-MS	AG	SG-E-DD[a,b]	SG-PM-HS	SG-PM-MS	SG-PM-MS	AG	SG-E-DD[a,b]	SG-PM-HS	SG-PM-MS	SG-PM-MS	AG	SG-E-DD[a,b]	SG-PM-HS	SG-PM-MS	SG-PM-MS
Dysprosium*[R]	0	6	4.3	5	17	0	NA	1	2	11	0	NA	1.2	2	11.3	0	NA	1.3	2	11.5
Manganese	780	790	550	500	600	780	790	550	500	600	780	790	550	500	600	780	790	550	500	600
Neodymium*[R]	0	28	35	42	155	0	NA	18	37	145	0	NA	17	34	128	0	NA	16	31	125
Nickel	410	340	420	442	410	410	340	420	442	410	410	340	420	442	410	410	340	420	442	410
Vanadium*	0	0	90	90	90	0	0	90	90	90	0	0	90	90	90	0	0	90	90	90

[a]For this technology type, there is no available prediction on its dysprosium and neodymium intensity. Therefore, the values reported for 2020 are used in the estimations.

[b]Values for SG-E-DD wind turbines are also used for HTS-DD as this is the most similar technology[20].

B.2: Resulting classifications

The scenarios considered for the estimation of material demands are presented in Table S9. While it appears in the manuscript, we have included it here to enhance the text coherence and simplify the review process.

Table S9: Classifications resulting by combining IAM capacity projections, market contributions, and material intensity scenarios.

Scenario	Market contribution	Intensity	Colour/symbol
C_B	Continued	Base	Red
C_L	Continued	Learning	Red (*)
T_B	Technological change	Base	Blue

T_L	Technological change	Learning	Blue (*)

B.3: Calculation of materials demands

To estimate the demand for materials, various factors such as projected technology capacities, the market contribution of technology types, materials intensity values, and technology learning curves are taken into account. The specific equation or method used to estimate material demand is not provided in the other relevant studies. However, we can calculate the material demand by multiplying the projected technology capacities (which already considers the effect of varying market shares) by material intensity values (with or without considering the impact of technology evolution on material intensity), as reported in Eq. S8.

$$MD^{T}_{m,t,n,s,k,i} = CCI^{T}_{t,n,s,k} \cdot MI_{m,t,n,i} \qquad \forall m,n,s,k,i,\ t \in TT_T,\ T = \{BAT, CSP, ELECTZ, PV, WIND\} \tag{S8}$$

Here, $MD^{T}_{m,t,n,s,k,i}$ is the demand for material *m* driven by technology type *t,* belonging to technology category *T*, at year *n* according to IAMs scenario s, market trend *k,* and material intensity *i* [ton]. $CCI^{T}_{t,n,s,k}$ is the capacity installed for individual type *t* of technology *T* at the year *n* according to IAMs scenario s and market trend *k* [GW] (as estimated in section A). $MI_{m,t,n,I}$ is the intensity *i* (e.g., base or with learning curves) of material *m* used in type *t* of technology *T* in year *n* [ton/GW]. The inclusion of set *n* in the material intensity accounts for the effect of varying material intensities over the years that might result from technology learning curves (as given by set *i*). Finally, the material demand considering all types *t* of technologies *T* can be aggregated to provide the lumped material demand of a given technology category (e.g., electrolyzers) for a specific scenario (combination of IAMs capacity projection, market trend, and material intensity), as given by $LMD^{T}_{m,n,s,k,i}$ in Eq. S9.

$$LMD^{T}_{m,n,s,k,i} = \sum_{t \in TT_T} MD^{T}_{m,t,n,s,k,i} \qquad \forall m,n,s,k,i \quad T = \{BAT, CSP, ELECTZ, PV, WIND\} \tag{S9}$$

Referring back to section B.2, it is important to note that depending on IAMs and market contribution scenarios, $CCI^{T}_{t,n,s,k}$ takes 50 different values for each technology type and year. Additionally, based on materials intensity scenarios, $MI_{m,t,n,I}$ assumes two different values for each technology type, material, and year. Consequently, we end up with 100 resulting values for both $MD^{T}_{m,t,n,s,k,i}$ and $LMD^{T}_{m,n,s,k,i}$.

B.4: Current production rate of materials, their reserve capacities, and production rate

To provide context for the material demands estimated, we compare them with the current production rates, as presented in Table S10. The information about data collection from the U.S. Geological Survey (USGS) and the specific webpage of USGS Commodity Statistics and Information. Generally, the production rates reported are based on values for 2020. However, in some cases the base year is later (i.e., 2021, or 2022), and, only in one case, it is 2018 (i.e., production rate of

praseodymium). In any case, there is no remarkable change in material reserve capacity or global production rate between 2020 and 2022.

Table S10: Annual production rate of the different materials.

Materials	Annual production rate [kton/year]	Ref.	Materials	Annual production rate [kton/year]	Ref.
Activated carbon	5700	[27]	Manganese	21500	[28]
Aluminium	65200	[28]	Molybdenum	298	[28]
Cadmium	25	[28]	Neodymium	21	[6]
Cement	4190000	[28]	Nickel	2240	[28]
Chromium	44000	[28]	Plastic	390700	[29]
Cobalt	132	[28]	Platinum	0.180	[28]
Concrete	4400000	[30]	Praseodymium	9.723	[28,31]
Copper	20300	[28]	Resin PPS - Glass fiber	5851	[32]
Dysprosium	1.800	[28,33]	Selenium	2.800	[28]
Gallium	0.327	[28]	Silica	266500	[34]
Glass	209000	[35]	Silicon	7000	[28]
Glass/Carbon composites/ fiberglass	5851	[32]	Silver	23.700	[28]
Gold	3.030	[28]	Steel	1958450	[36]
Graphite	966	[28]	Tellurium	0.470	[28]
Indium	0.957	[28]	Terbium	0.340	[28,37]
Iridium	0.004	[28,38]	Titanium	7600	[28]
Iron	1300000	[28]	Vanadium	105	[28]
Lithium	77	[28]	Zinc	13000	[28]

We also present Table S11 and S12, reporting the capacity of the reserves for minerals and their current recycling rate that will be used later in section B.7 and section C which dedicated to our optimization models.

Table S11: Capacity of the reserves for different materials.[28]

Mineral	Reserve capacity [ton]	Mineral	Reserve capacity [ton]
Aluminium	$3 \cdot 10^{10}$	Manganese	810,000,000
Cadmium	600,000	Molybdenum	18,000,000
Chromium	570,000,000	Neodymium	8,000,000
Cobalt	7,000,000	Nickel	89,000,000
Copper	$8.7 \cdot 10^{8}$	Platinum	69,000
Dysprosium	1,410,000	Praseodymium	4,000,000
Gallium	279,300	Selenium	99,000
Gold	50,000	Silver	560,000

Graphite	$3 \cdot 10^8$	Tellurium	31,000
Indium	5,700	Terbium	$1.2 \cdot 10^8$
Iridium	69,000	Titanium	47,000,000
Iron	$8.1 \cdot 10^9$	Vanadium	22,000,000
Lithium	17,000,000	Zinc	250,000,000

Table S12: Current recycling rate for different materials.[28,39]

Mineral	Recycling rate* [%]	Mineral	Recycling rate* [%]	Mineral	Recycling rate* [%]
Cadmium	17.5	Indium	37.5	Praseodymium	5.5
Cobalt	37.5	Iridium	17.5	Selenium	5.5
Copper	34	Lithium	1	Silicon	-
Dysprosium	5.5	Manganese	56	Silver	37.5
Gallium	17.5	Neodymium	5.5	Tellurium	-
Graphite	-	Nickel	50	Terbium	1

* It is defined as the fraction of secondary metal in total metal input in metal production process.[39]

B.5: Exploring the possibilities of by-products

For a comprehensive understanding of the dynamics between host elements and their associated by-products, it is vital to consider the broader context and competing demands from different sectors and applications. Here, we estimate the by-product production that would be obtained when sourcing the host elements to develop CETs. Table S13 presents the companion elements and the parameters used to estimate the amount of by-product produced. Notably, the column "dependency" in this table presents the percentage of guest that is currently product as a by-product of its host at global scale. This value, which is not directly used in the calculations, is presented as an indicator of the strength of the relationship between each pair of elements.

Depending on data availability, one of the Eqs. S10-S12 is employed to calculate the resulting amount of by-product that will be obtained as a result of mining the host element. This is indicated in the last column of Table S13.

Table S13: Companion elements and their relevant data.

Guest	Host	Dependency[a,b] [%]	Concentration of guest in concentrated host ($^{CGCH_{g,m}}$)	Concentration of guest in the host's ore (^{CGOre_g})	Relative concentration of guest to host in their ore [%] $\left(\frac{^{CGOre_g}}{^{CHOre_g}}\right)$	Ore to metal ratio (^{OreMR_m}) [40]	Recovery rate [%] ($^{RR_{g,m}}$)	Equation used
Cadmium	Zinc	90 [41]	0.4% [42]	-	-	-	94 [42]	S10
Gallium	Aluminium	95 [28]	-	50 ppm[28]	-	4.2	10 [28]	S11
Gallium	Zinc	-	-	<50 ppm[28]	-	52.8	10 [28]	S11
Indium	Zinc	75 [41]	-	1-100 ppm[28]	-	52.8	(100)[c]	S11
Iridium	Platinum	98 [41]	-	-	7 over 92.55 [43]	-	(100)[c]	S12
Silver	Zinc	40 [41]	-	-	$116.32 \cdot 10^{-4}$ over	-	(100)[c]	S12

					6.49 [44]			
Silver	Copper	25 [41]	100 - 700 ppm [45]	-	-	-	(100)[c]	S10

[a]Global production percentage of host element derived as a by-product of its host element.

[b]It is reported to demonstrate the dependency between the production of the guest and the host elements, although it is not directly used in any calculations.

[c]In the absence of reported data, it is assumed to be 100%.

$$PG_{g,n,s,k,i} = \sum_{m \in HOST_g} \left(\sum_{T} LMD^{T}_{m,n,s,k,i} \cdot CGCH_{g,m} \cdot RR_{g,m} \right) \qquad \forall g,n,s,k,i \qquad \text{(S10)}$$

$$PG_{g,n,s,k,i} = \sum_{m \in HOST_g} \left(\sum_{T} LMD^{T}_{m,n,s,k,i} \cdot OreMR_m \cdot CGOre_g \cdot RR_{g,m} \right) \qquad \forall g,n,s,k,i \qquad \text{(S11)}$$

$$PG_{g,n,s,k,i} = \sum_{m \in HOST_g} \left(\sum_{T} LMD^{T}_{m,n,s,k,i} \cdot \frac{CGOre_g}{CHOre_g} \cdot RR_{g,m} \right) \qquad \forall g,n,s,k,i \qquad \text{(S12)}$$

Here, $^{PG}_{g,n,s,k,I}$ is the amount of guest element *g* that would be produced at year *n*, according to IAMs scenario s market trend k and materials intensity i [ton], $^{LMD^{T}}_{m,n,s,k,i}$ is the demand for material *m* which is the host for element *g* (as given by set $^{HOST}_{g}$) driven by all the technology types in category *T* at year *n* [GW], as estimated in section B.4, and $^{RR}_{g,m}$ is the recovery rate of guest element *g* from its host element *m* [%]. Apart from these parameters, that are common between the three equations, each equation has a specific parameter. The term $^{CGCH}_{g,m}$ is the concentration of guest *g* in concentrated host *m* [%], while $^{CGOre}_{g}$ is the concentration of guest *g* in the ore [ppm], $^{OreMR}_{m}$ is the ore to metal ratio [ton_{ore}/ton_{metal}], and $^{CHOre}_{m}$ is the concentration of the host *m* in the ore [ppm].

B.6: Estimated material demands

We computed annual demands for 36 materials (Table S5) across 25 IAM scenarios (Table S2), and four categories (Table S9), with minimum and maximum values presented in Tables S14-S15. In Table S16, we compared our estimated range with a recent study[6], and with IEA data explorer, where data are available. Also, Figure S3 visualizes 20 materials with demand-to-production ratios below one.

Table S14: Materials annual demand, based on minimum values across scenarios [ton].

Materials	2020	2025	2030	2035	2040	2045	2050
Activated carbon	0.0	0.0	0.0	0.0	0.0	0.0	0.1
Aluminium	63290.8	56571.7	3919.9	135354.0	405027.6	791845.1	732071.0
Cadmium	6.7	15.8	1.1	31.2	55.6	100.9	93.5
Cement	388735	196925	4194.9	146888	2946016	6157336	5537179
Chromium	3053.0	1299.2	0.0	0.0	25928.8	54023.4	45637.5
Cobalt	0.0	0.0	16059.1	12597.3	9393.4	10340.4	4502.3
Concrete	2969770	1503798	31795	1095223	22293525	46518098	41627387
Copper	48130.5	38555.5	2450.0	84357.9	322257.2	637239.2	588959.3
Dysprosium	30.6	11.5	0.0	0.0	193.6	402.4	339.2
Fiberglass	53197.1	22958.8	0.0	0.0	453504.3	933548.7	779292.8
Gallium	0.2	0.2	0.0	0.4	1.0	1.6	1.3
Glass	218985	322916	24336	836430	2063664	3854748	3687399
Gold	0.0	0.0	0.0	0.0	0.0	0.0	0.0
Graphite	0.0	0.0	0.0	0.0	0.0	0.0	0.0
Indium	2.0	3.3	0.2	4.9	7.7	11.4	7.9
Iridium	0.0	0.0	0.0	0.0	0.0	0.0	0.0
Iron	114283.1	48535.5	0.0	0.0	965745.3	2011225.5	1698261.7
Lithium	0.0	0.0	15317	15037	15890.7	27647.5	31020.2
Manganese	4824.4	2350.6	191.2	3823.1	42702.6	90147.1	93413.5
Molybdenum	631.2	268.5	0.0	0.0	5356.1	11158.6	9425.7
Neodymium	170.4	65.9	0.0	0.0	1144.4	2369.3	1986.1
Nickel	2606.3	1286.3	50.3	956.9	23149.1	48127.0	43834.3
Plastic	112170.1	82230.5	4518.8	155371.1	824399.7	1645356.1	1517297.1
Platinum	0.0	0.0	0.0	0.0	0.0	0.0	0.0
Praseodymium	41.3	17.2	0.0	0.0	330.5	684.7	575.2
Resin	0.0	0.0	0.0	0.0	0.0	0.0	1.0
Selenium	1.8	2.4	0.2	4.3	7.7	12.7	10.6
Silica	0.0	0.0	1819.6	1789.6	1818.0	3147.4	3430.7
Silicon	17745.3	21414.0	1242.7	37732.3	81360.1	133610.1	111151.3
Silver	79.9	98.3	7.0	150.7	229.5	388.6	308.6
Steel	1048043	732636	36967	1249165	8065432	16187947	14874057
Tellurium	7.2	15.1	0.9	28.5	60.6	109.5	101.0
Terbium	5.6	2.4	0.0	0.0	47.4	98.6	83.3
Titanium	0.0	0.0	0.0	0.0	0.0	0.0	0.3
Vanadium	167.1	77.8	0.2	3.2	1731.9	3669.1	3159.2

Zinc	36372.7	15708.7	0.0	0.0	310220.7	638300.1	532582.9

Table S15: Materials annual demand, based on maximum values across scenarios [ton].

Materials	2020	2025	2030	2035	2040	2045	2050
Activated carbon	58.8	106.7	199.1	739.1	1439.6	3867.9	7392.8
Aluminium	1812202	4791170	9690448	13260975	15370312	17341446	18865155
Cadmium	435.1	2029.7	5780.8	10113.6	14142.1	17655.3	21379.0
Cement	5546556	22499308	22584053	33490551	33485745	31520519	30995030
Chromium	39467.2	197658.5	203658.8	275285.4	280031.5	220114.3	298248.7
Cobalt	72145.6	44630.8	255440.7	337313.5	403271.7	646266.6	800623.1
Concrete	42552544	171674480	172318684	256402911	256366393	243276922	239436170
Copper	1160247	3197534	5692857	7797968	9009154	9576423	10004045
Dysprosium	445.9	2423.6	2682.0	4133.6	4704.5	3386.0	4176.3
Fiberglass	649475	3157588	3161239	4203255	4207135	3264965	4368525
Gallium	7.9	68.5	203.2	397.7	595.5	726.3	864.5
Glass	8554225	26492213	47140203	65908593	76747704	80235609	83570669
Gold	1.3	2.4	4.5	16.8	32.7	87.8	167.8
Graphite	228919	190830.9	1429555	1818315	2095153	3357108	4169166
Indium	106.9	650.9	1889.7	3494.3	5061.4	6242.5	7492.5
Iridium	4.0	7.2	13.5	50.0	97.5	261.8	500.4
Iron	1454362	7270284	7477996	10133718	10333703	8106797	10963575
Lithium	37487.0	31918.5	255259.4	387581.9	518810.1	951188.5	1325084
Manganese	118242	280282.9	425237.7	541609.1	638782.2	952438.9	1180557
Molybdenum	8136.9	40737.6	41961.2	56744.9	57748.7	45376.4	61462.7
Neodymium	3292.8	18970.0	21949.7	34972.7	40787.6	28804.6	34732.3
Nickel	158359	192178.1	1270745	1654463	1948754	3197836	4178685
Plastic	2235640	6222393	10822731	14796901	17070479	17881345	18430439
Platinum	1.1	2.1	3.8	14.2	27.7	74.4	142.2
Praseodymium	646.6	3658.9	4177.7	6857.8	8165.9	5670.5	6696.1
Resin	614.9	1116.7	2082.7	7731.8	15060.7	40464.5	77339.9
Selenium	71.9	668.0	1981.1	3877.8	5805.7	7081.1	8429.1
Silica	4606.4	3774.2	28284.0	35955.7	41417.2	66490.6	82668.6
Silicon	707936	2146783	3819982	5340869	6219211	6501851	6772106
Silver	3194.8	9661.8	17189.9	24033.9	27991.5	29436.5	30538.1
Steel	20500420	60788239	95375058	129796162	149790125	155726664	157464932
Tellurium	470.1	2183.9	6217.6	10866.4	15184.1	18960.9	22963.9
Terbium	119.3	706.7	834.0	1383.5	1659.2	1145.8	1343.5
Titanium	153.7	279.2	520.7	1932.9	3765.2	10116.1	19335.0

Vanadium	4354.6	24314.5	27486.0	39320.9	42129.6	31796.1	41353.2
Zinc	443452	2153462	2153462	2860649	2860649	2218995	2967649

Table S16: Comparison of estimated values with similar studies.

Material	comparison with similar studies [6]	Comparison with "IEA data Explorer" [46]	Reason
Ag	OV_U	√	
Al	OV_L	-	
Cd	OV	√	
Cem.	OV_L	-	
Co	-	√	
Cr	-	√	
Cu	-	√	
Dy	X	√	Electric motors and in turn the demand driven by them is not included in our study.
Ga	X	√	It is used in certain types of PV panels, and variations in its demand are possible depending on the capacity assigned to each type
GCC	OV_L	-	
Gla.	OV_U	-	
Gra.	-	√	
In	X	√	It is used in certain types of PV panels, and variations in its demand are possible depending on the capacity assigned to each type
Ir	-	√	
Li	-	√	-
Mn	OV_U	√	
Mo	-	√	
Nd	X	√	Electric motors and in turn the demand driven by them is not included in our study.
Ni	X	√	Electric motors and in turn the demand driven by them is not included in our study.
Pt	-	√	
Pr	-	√	
Se	X	√	It is used in certain types of PV panels, and variations in its demand are possible depending on the capacity assigned to each type
Si	-	√	
Ste.	OV_L	-	
Te	X	√	It is used in certain types of PV panels, and variations in its demand are possible depending on the capacity assigned to each type

Tb	-	√	
V	-	√	
Z	-	√	

OV_U: There is considerable overlap in the range of estimations, and our estimate represents a conservative upper bound.

OV_L: There is considerable overlap in the range of estimations, and our estimate represents a conservative lower bound.

X: While there are some overlaps in the data, it does not seem enough to consider them at the same range.

√: While the ranges provided may not align precisely, they exhibit striking similarity. It is noteworthy that for certain elements, like those used in the electrolyzers, while the IEA's range follows an inverted U-shaped pattern, our estimations derived from IAMs consistently show a rising trend.

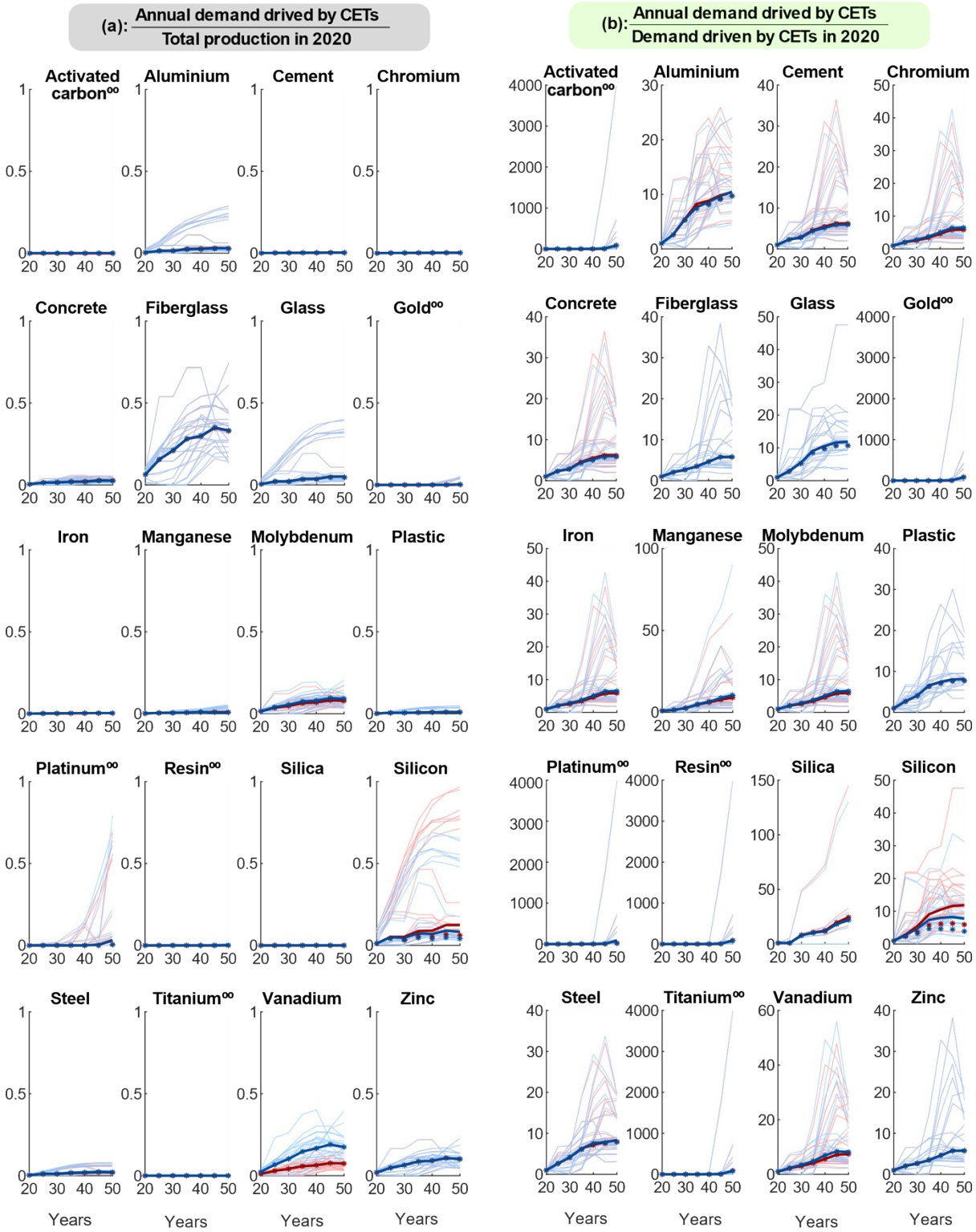

Fig.S3 Material demands from clean energy technologies. Panel (a) compares the demand for materials from CETs with their production rate dedicated to all sectors in 2020. Panel (b) represents materials demand from CETs compared with their estimated demand in 2020. ^{OO}: Materials primarily used in electrolyzers, does not exhibit demand until 2030 and therefore rely on this year or later years, depending on the scenario, as the basis for calculations. Timeframes are indicated as follows: 20: 2020, 30: 2030, 40: 2040, 50: 2050. The results of the continued trend and technological change are distinguished by red and blue colors, respectively. In both cases, the median is depicted with a thicker line. The effect of the reductions in material intensities due to learning curves is indicated with star signs, only for median projections. CETs: clean energy technologies.

B.7: Links between problematic materials and technology types

Figure S4 presents the intricate relationships among different types of clean energy technologies and materials, addressing potential challenges in terms of supply and pricing. On the right side, we list various technology types contributing to the 2050 market, with box widths indicating their reliance on featured materials compared to other technologies. On the left side, we show problematic materials highlighted (i.e., those whose demand-to-production ratio is more than 0.5). The ribbons in the figure represent connections between materials and their respective technology hosts, affected by technologies learning curve. Shortages or price increases in these materials may impact the development and market penetration of the associated CETs.

Fig.S4 corresponds to Fig.5 in the main manuscript, illustrating the connections between materials and clean energy technologies for the years 2050 and 2020, respectively. It is important to note that in both figures, the intensity values are normalized, meaning that the intensity value for each material is divided by the largest intensity value for that year.

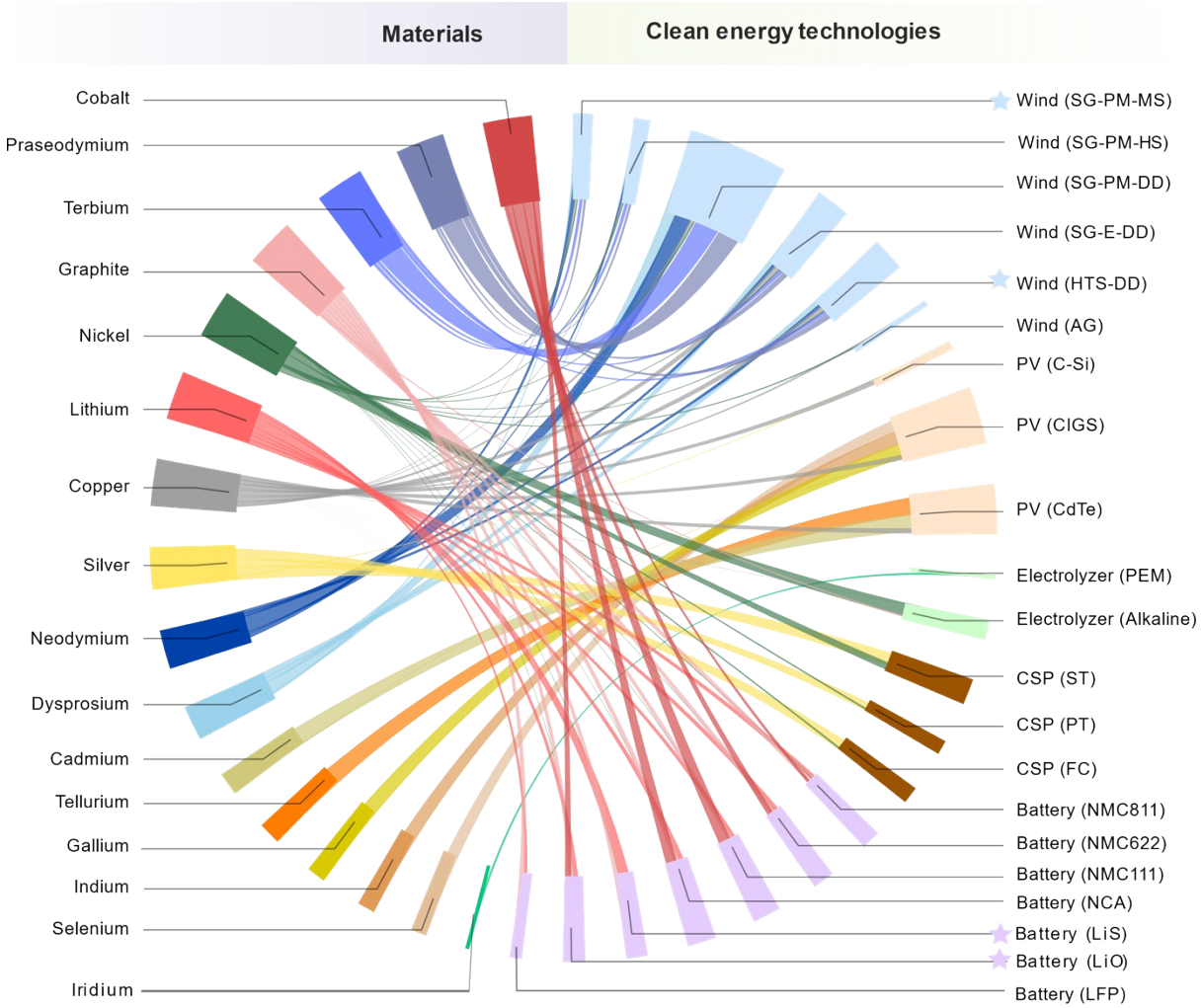

Fig.S4 Links between the materials (left-hand side) and clean energy technologies (right-hand side), based on material intensity values in 2050, considering the effect of learning curves. The width of the ribbons is proportional to material intensity values. Technologies that penetrate the market after 2020 are distinguished by a star. Note that to make all the materials visible and comparable with 2020 values, the materials relative to 2020 intensity values are normalized. For clarity, technology types are enclosed in brackets, with the corresponding acronyms found in Table S1.

B.8: Demand-to-reserves comparison

We also made a comparison between the demand values of materials and their reserve capacities (refer to Table S11). We found that cobalt, indium, selenium, silver, and tellurium exhibited a demand-to-reserve ratio potentially exceeding one in some scenarios. Additionally, cadmium, copper, lithium, nickel, and zinc although display demand-to-reserve ratios smaller than one, are noteworthy. Figure S5 illustrates these minerals.

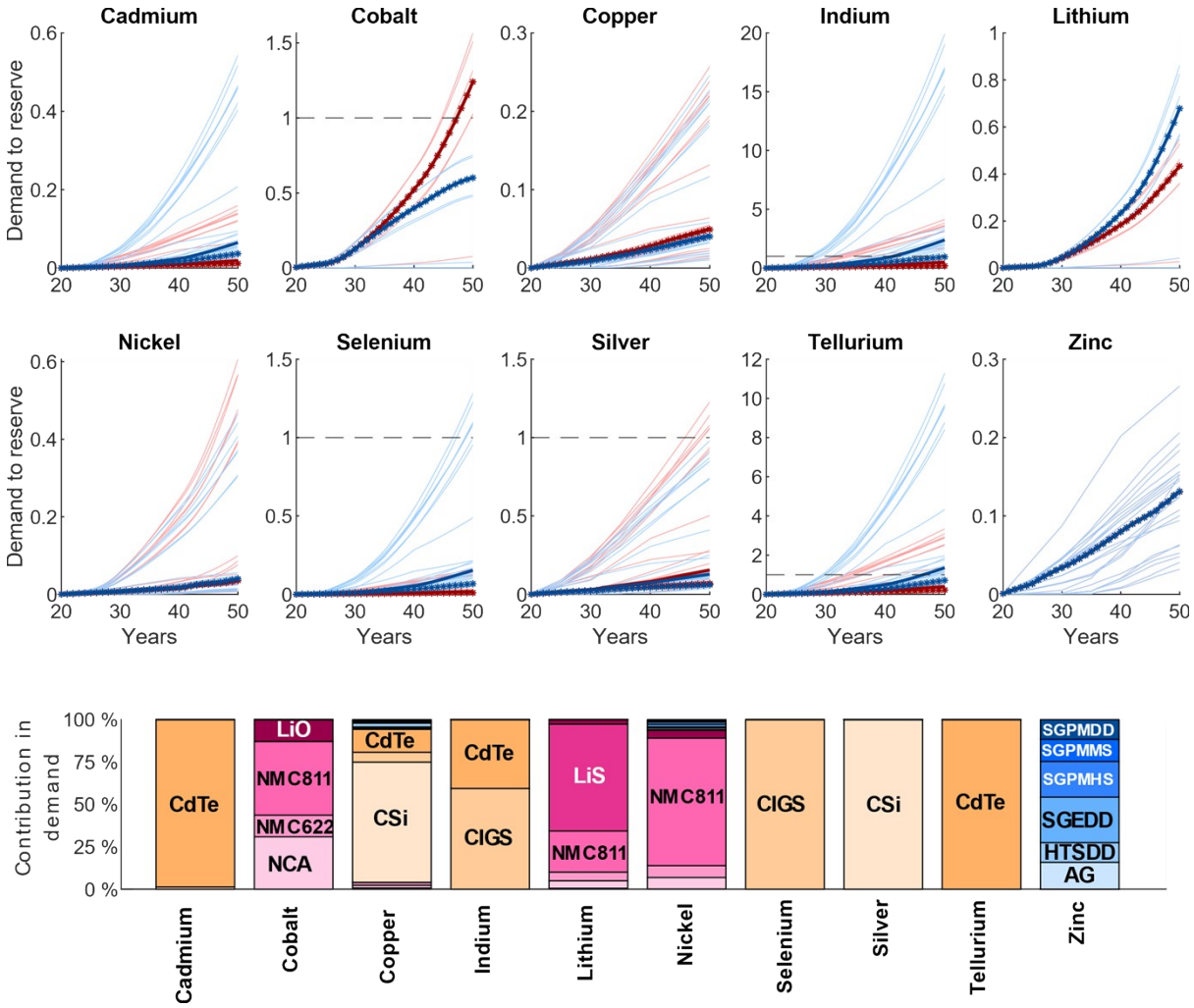

Fig.S5 Materials demand over their reserve capacities. To aid comparison, dashed horizontal lines are included. Timeframes are indicated as 20: 2020, 30: 2030; 40: 2040, 50: 2050. The results of the continued trend and technological change are distinguished by red and blue colors, respectively. In both cases, the median is depicted with a thicker line. Additionally, the resulting median, accounting for reductions in materials intensity based on learning curves, is indicated by star signs. The stacked bars chart presents the share of different technology types in specific material demands. Technology type acronyms as given in Table S1.

C: Optimization model to estimate realistic capacities

This section is dedicated to estimating the achievable capacity of clean energy technologies while accounting for constraints on materials availability. Additionally, we calculate the necessary recycling rates of materials to meet their projected capacity by IAMs. The steps involved are as follows:

- C.1: Estimating shortages in technologies developed capacity: Utilizing the projected capacity of technologies by IAMs as a starting point, we impose constraints based on materials reserve capacity and allocated demand to reassess their achievable capacity and compare them with IAMs projections.

- C.2: Estimating required recycling: Taking into account similar constraints, we estimated the required recycling range for each of the materials needed to meet the capacity of clean energy technologies as projected by IAMs.

C.1: Estimating shortages in technologies developed capacity

Previous analyses suggest that IAM projections on the of CETs are probably too optimistic when factoring in material supply rates, and a higher technological resolution. To assess how far these might be from reality, we evaluate the capacity of CETs that could be realistically deployed considering material availability. To this end, we formulate an optimization model (M1) to minimize the disparity in capacities between IAM projections and what could be realistically manufactured. In all the equations, variables are written in *italics* while parameters are in normal style.

Model M1: minimizing disparities

$$Min \sum_{T,n,s} Diff_{n,s}^{T} \quad \text{(S13)}$$

$$s.t: \quad Diff_{n,s}^{T} = \sum_{t \in TT_t} \left(CCI_{t,n,s}^{T,Opt} \right) - CC_{n,s}^{T,IAMs} \qquad \forall n,s,T = \{BAT, CSP, ELECTZ, PV, WIND\} \quad \text{(S14)}$$

$$Diff_{n,s}^{T} \geq 0 \qquad \forall n,s,T = \{BAT, CSP, ELECTZ, PV, WIND\} \quad \text{(S15)}$$

$$\sum_{T,t} CCI_{t,n,s}^{T,Opt} \cdot MI_{m,t,n} \leq PR_{m,n} \cdot SHARE_{m,2020}^{CETs} \qquad \forall m,s,n = 2021, \ldots, 2050 \quad \text{(S16)}$$

$$\sum_{t,n,T} CCI_{t,n,s}^{T,Opt} \cdot MI_{m,t,n} \leq Res_m \qquad \forall m,s \quad \text{(S17)}$$

$$Diff_{n,s}^{T}, CCI_{t,n,s}^{T,Opt} \in R^{+} \qquad \forall n,s,t,T = \{BAT, CSP, ELECTZ, PV, W \quad \text{(S18)}$$

The objective of M1 (Eq. S13) is to minimize the disparities in capacity across different technology categories *T* (e.g., PV), IAMs scenario s, and years *n*, as denoted by $Diff_{n,s}^{T}$. These disparities are quantified in Eq.S14 as the difference between the capacity assigned to each technology based on IAM projections ($CC_{n,s}^{T,IAMs}$) and the "realistic" estimates obtained with this model ($\sum_{t} CCI_{t,n,s}^{T,Opt}$). For each technology, this difference should be positive to ban situations where excess capacity for a technology

category compared with IAMs projections offsets deficits for other categories (Eq. S15). $CC^{T,IAMs}_{n,s}$ is obtained with Eqs. S2-S6, for the corresponding IAM scenario and material intensity values.

We acknowledge that not all the materials produced can be allocated to the development of CETs since they are also used in other sectors. Hence, we restrict the amount of each material that can be used for manufacturing CETs according to the shares observed in 2020 ($SHARE^{CETs}_{m,2020}$). Hence, the left-hand side of Eq. S16 estimates the demand for material *m* driven by all types of technology *T* developed at year *n*, by multiplying the capacity of each technology type by its material intensity ($MI_{m,t,n}$), while the right-hand side accounts for the (share of) the realistic production rate that is expected for material *m* in year *n* ($PR_{m,n}$). As aforementioned, the available share of each material *m* is obtained based on 2020 values (Eq. S19).

$$SHARE^{CETs}_{m,2020} = \frac{\sum_{t,T} CCI^{T,IAMs}_{t,2020} \cdot MI_{m,t,2020}}{PR_{m,2020}} \qquad \forall m,n = 2021, \ldots,2050 \tag{S19}$$

Capacity projections and material intensities are set at appropriate values depending on the corresponding scenario studies, while production rates for 2020 ($PR_{m,2020}$) are detailed in Table S10. Exceptionally, for iridium, used in electrolyzers, we conducted the estimation based on the initial year of the technology (i.e., after 2030, depending on the IAM scenario), instead of in 2020.

The production rates for future years appearing in Eqs. S16 and S19 ($PR_{m,n}$) are obtained by allowing a certain annual growth α, starting from the production rate of 2020 (see Eq. S20). Specifically, we used α = 2.7%, which is the average annual growth of metals mining [47], and changed this value to 0.7 and 4.7 for the sensitivity analysis. (i.e., average ± 2%).

$$PR_{m,n} = (1+\alpha) \cdot PR_{m,n'} \qquad n' = (n-1), \forall n = 2021, \ldots,2050 \tag{S20}$$

Finally, Eq.S17 is employed to restrict the cumulative demand for material *m* by year *n* driven by all the technologies according to the capacity of its reserves (Res_m), as given in Table S11.

Notably, by combining three production rates with two materials intensity projections, six sets of results are created for each of the 25 IAMs scenario. Figure S6 presents the median shortage values for each set and each IAM scenarios.

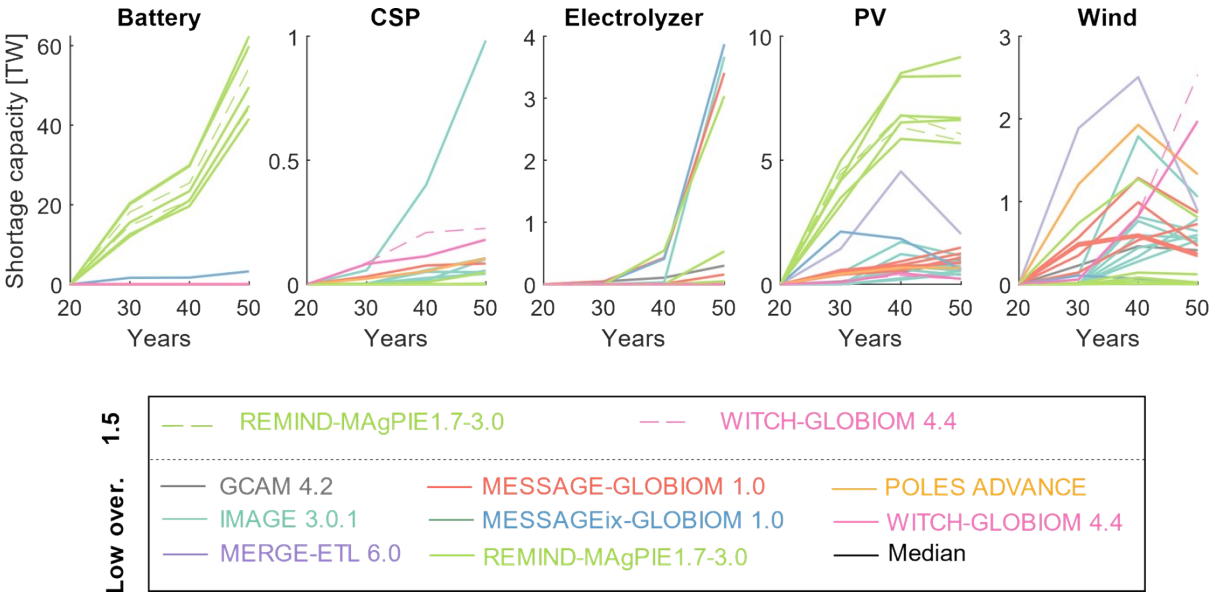

Fig.S6 Shortages in technologies annual developed capacity based on different IAMs scenarios.

C.2: Estimating required recycling:

To assess the minimum recycling rate for materials to meet the demand from CETs, we construct another model with similar constraints. This aids in understanding the significance of materials recycling and gauging the disparity between our expectations and their current recycling rates (see Table S12). For this purpose, we formulate an optimization model (M2) aimed at minimizing the recycling rate required for materials to fulfil IAM's projected capacities. In all equations, variables are denoted in italics while parameters are in normal style.

Model M2: minimizing recycling rates

$$Min \sum_{i,n,s} Rec_{i,n,s} \tag{S21}$$

$$\sum_{T,t} CCI^{T,Opt}_{t,n,s} \cdot MI_{m,t,n} \leq PR_{m,n} \cdot SHARE^{CETs}_{m,2020} + Rec_{i,n,s} \qquad \forall m,s,n = 2021, \ldots,2050 \tag{S22}$$

$$\sum_{t,n,T} CCI^{T,Opt}_{t,n,s} \cdot MI_{m,t,n} \leq Res_m + Rec_{i,n,s} \qquad \forall m,s \tag{S23}$$

$$CCI^{T,Opt}_{t,n,s} = CCI^{T,IAMs}_{t,n,s} \qquad \forall n,s,t,T = \{BAT, CSP, ELECTZ, PV, WIN \tag{S24}$$

$$Rec_{i,n,s}, CCI^{T,Opt}_{t,n,s} \in R^{+} \qquad \forall n,s,t,T = \{BAT, CSP, ELECTZ, PV, WIN \tag{S25}$$

Model M2, outlined in equations (S21) to (S25), seeks to minimize the material recycling across materials intensity projections i, IAM scenarios *s,* and years *n*. The objective (Eq. S21) aims to minimize the recycled materials indicated by $Rec_{i,n,s}$, while considering IAM projections. This term is incorporated into the right-hand side of Eqs. S22 and S23 to increase material availability. Eqs. S22 and S23 are equivalent to Eqs. S16 and S17 in model M1. However, in model M2, we enforce the exact capacity values based on IAM projections through Eq. S24. Not that the $CCI^{T,IAMs}_{t,n,s}$ contains the market contribution trends (see Eq.S7).

It is important to note that, for each material *m* and IAM scenario *s*, 12 sets of results are obtained, each considering one of three production rates, one of two material intensity projections, and one of two market contribution trends. This comprehensive approach allows for a thorough assessment of the recycling rates required across various scenarios and parameters.

D: Extra warming due to shortages in technology developed capacities

Our optimization model highlights a potential challenge: achieving the capacities projected by IAMs for 1.5°C and 1.5°C with low overshoot temperature targets may be constrained by material supply. This section delves into estimating the additional warming that could result from these shortages. Here, "shortage" denotes the disparity between the capacity projected by IAMs and the more realistic capacity that could be deployed according to our model. It is important to note that electrolyzers are excluded from this analysis as we conservatively assume that the hydrogen generated would be utilized in chemical industries (i.e., not for energy applications). The steps involved in this estimation are outlined below:

- **D.1: Expected energy delivered:** First, we estimate the energy that could be delivered by CETs if we could achieve the capacity projected by IAMs.
- **D.2: Real energy delivered:** Then, we calculate the energy that can be delivered by the capacity of technologies obtained from our optimization model, which includes constraints on material supplies.
- **D.3: Replacement energy:** The difference between the energy expected to be delivered and that actually delivered should be substituted by alternative sources.
- **D.4: Additional greenhouse gas emissions:** Shortages in the capacity developed for CETs requires contributions from business-as-usual sources for compensation. Specifically, we assume the electricity mix would supply shortages in CSP, PV and wind capacity, while diesel-engine trucks would replace missing EVs due to shortages in the capacity of batteries. This substation would result in the release of additional CO_2-eq emissions compared to the original IAM estimates. To quantify them, we resort to prospective life cycle assessment.
- **D.5: Additional warming:** We translate non-avoided CO_2-eq emissions into additional warming.

Each step is discussed in detail in the following sections.

D.1: Expected energy delivered

To estimate the amount of energy delivered (ED) by all the capacity installed in each year for all technologies during their lifetime, Eqs. S26-S27 have been employed.

$$ED^{BATEV,IAMS}_{n,s} = CC^{BATEV,IAMs}_{n,s} \cdot \frac{REC^{BAT}}{RPC^{BAT}} \cdot OCLT^{BAT} \cdot DOD^{BAT} \cdot RTEff^{BAT} \qquad \forall n,s \qquad \text{(S26)}$$

$$ED^{T,IAMs}_{n,s} = CC^{T,IAMs}_{n,s} \cdot GCF^{T} \cdot \left(\frac{365\ days}{year} \cdot \frac{24\ h}{day} \cdot LF \right) \qquad \forall n,s, T = \{CSP, PV, WIND\} \qquad \text{(S27)}$$

The term $ED^{BATEV,IAMS}_{n,s}$ used in Eq. S26 indicates the energy delivered by installed capacity of batteries according to IAMs scenario *s* in year *n* [GWh]. In this equation, REC^{BAT} is the rated energy capacity of batteries [GWh], while RPC^{BAT} is its rated power capacity [GW]. These parameters represent the nominal energy or power output of a battery in each cycle, respectively. Here, the ratio of 20/6 is used as rated energy-to-rated power capacity of batteries[48]. $OCLT^{BAT}$ is the number of operational cycles

expected during the lifetime of the battery (e.g., 3000 cycles during 15 years). Then, DOD^{BAT} is the depth of discharge, providing the amount of energy discharged compared with the total storage capacity (e.g., 80%). $RTEff^{BAT}$ denotes the battery round-trip efficiency, which reflects the efficiency (%) achieved through converting electricity from alternating current to stored energy and back to alternating current (e.g., 86%) [5]. Finally, $CC^{BATEV, IAMs}_{n,s}$ is the annual capacity of batteries used in EVs [GW], estimated from IAM projections using Eqs. S3-S5.

$ED^{T, IAMs}_{n,s}$ in Eq. S27 represents the energy delivered from the capacity of CSP, PV or wind installed in year *n* according to IAM scenario *s* [GWh]. In this equation, GCF^{T} is the global capacity factor for the desired technology [%], equal to 32.8% for wind and 22.4% for PV[49]. For CSP, the value of 45% related to CSP systems with thermal storage is used[50]. Also, LF is the lifespan, which is assumed to be 30 years for these technologies. $CC^{T, IAMs}_{n,s}$ is the capacity of each technology installed in year *n* [GW], which is directly reported by IAMs for CSP, PV, and wind.

We aim to emphasize that our goal in conducting these estimations is to calculate the additional warming resulting from capacity shortages and add it into the initial target of limiting global warming to 1.5°C by 2100. Hence, even if part of the energy generated by some technologies installed in the 2020-2050 will occur after 2050, it will still occur before 2100 (note the lifespan of 30 years). Thus, this approach is relevant and meaningful in this context.

D.2: Real energy delivered

Analogous to the estimation of the expected energy delivered, we calculate the amount of energy that would be delivered in practice during the lifetime of the technologies installed with the available capacity according to the optimization model (Eqs. S28-S29). The only difference compared with Eqs. S26 and S27 is the replacement of the capacities obtained by the IAMs by those obtained from model M1 (see section C).

$$ED^{BATEV,Opt}_{n,s} = CC^{BATEV,\,Opt}_{n,s} \cdot \frac{REC^{BAT}}{RPC^{BAT}} \cdot OCLT^{BAT} \cdot DOD^{BAT} \cdot RTEff^{BAT} \qquad \forall n,s \qquad \text{(S28)}$$

$$ED^{T,Opt}_{n,s} = CC^{T,\,Opt}_{n,s} \cdot GCF^{T} \cdot \left(\frac{365\ days}{year} \cdot \frac{24\ h}{day} \cdot LF \right) \qquad \forall n,s\ T = \{CSP, PV, WIND\} \qquad \text{(S29)}$$

The term $ED^{BATEV, Opt}_{n,s}$ used in Eq. S28 indicates the energy delivered by the capacity of batteries according to scenario *s* installed in year *n* according to the optimization model [GWh], while $ED^{T, Opt}_{n,s}$ in Eq. S29 represents the same for CSP, PV, or wind [GWh].

As discussed in the previous section, our aim is to calculate the additional warming and add it into the target of limiting global warming to 1.5°C by 2100, even for technologies installed close to 2050, as the energy they will generate will be expended by 2100.

D.3: Replacement energy

To estimate the amount of energy that could not be delivered because of shortages in the capacity of each technology and needs to be provided by business-as-usual options, we employ Eqs. S30-S32.

$$SED_{n,s}^{BATEV} = ED_{n,s,k,i}^{BATEV,IAMS} - ED_{n,s}^{BATEV,Opt} \qquad \forall n,s \qquad \text{(S30)}$$

$$MSED_{n,s}^{T} = ED_{n,s}^{T,IAMs} - x_n^T \cdot SED_{n,s}^{BATEV} \qquad \forall n,sT = \{CSP,PV,WIND\} \qquad \text{(S31)}$$

$$SED_{n,s}^{T} = MSED_{n,s}^{T} - ED_{n,s}^{T,Opt} \qquad \forall n,s\ T = \{CAP,PV,WIND\} \qquad \text{(S32)}$$

Eq. S30 is used for batteries, with the term $SED_{n,s}^{BATEV}$ [GWh] representing the substitute energy that should be delivered in year *n* to compensate for the capacity that could not be developed owing to shortages in material supplies. Parameters $ED_{n,s}^{BATEV,IAMS}$ and $ED_{n,s}^{BATEV,Opt}$ are estimated using Eq. S26 and Eq.S28, respectively.

We could use the same approach for the case of CSP, PV, and wind. However, we adopt a conservative approach and assume that part of the capacity that was projected for CSP, PV, and wind by IMAs was going to be dedicated to batteries used in EVs. Hence, if the expected capacity of batteries (and consequently EVs) could not be developed, there is also no need to develop the corresponding capacity of CSP, PV panels, and wind turbines required to feed them. To account for this, we introduce Eq. S31, where we deduct the energy that does not need to be delivered anymore owing to the shortage in batteries. To allocate this capacity between CSP, PV, and wind the term x_n^T is used to reflect the contribution of each of these technologies in feeding the batteries. This value is given by the share of CSP, PV, and wind capacities in year *n* according to IAM estimates. At the end, the equation estimates the "modified" replacement energy that needs to be delivered according to IAMs scenario s in year *n* ($MSED_{n,s}^{T}$). $SED_{n,s}^{T}$ in Eq. S32 represents the energy that could not be supplied by CSP, PV panels, or wind turbines because of material shortages, and, therefore, should be replaced by the grid in each year *n* [GWh]. Finally, $ED_{n,s}^{T,Opt}$ and $MSED_{n,s}^{T}$ are estimated using Eqs. S29 and S31, respectively. Fig. S7 depicts this approach.

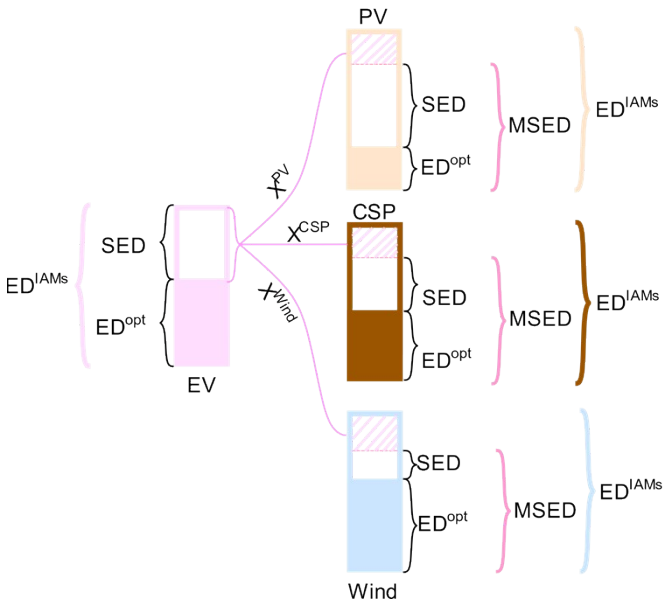

Fig.S7: Approach used to estimate the replacement energy requirements for each clean energy technology.

D.4: Additional greenhouse gas emissions

In order to calculate the extra greenhouse gas emissions, it is important to note that IAMs anticipate a specific level of emissions for the projected capacity of clean energy technologies for a particular temperature target. Indeed, their projections are based on expected emission levels. Therefore, to estimate the additional emissions, we need to determine the difference between their expected emissions and the emissions that would occur based on the realistic capacities derived from our optimization model (Section C). We also consider the services, such as transportation or electricity, that these technologies would provide but they cannot due to capacity shortages (i.e., difference between IAMs and optimized capacities). We replace these unmet services with equivalent options and estimate the corresponding resulting emissions, which are included in our additional greenhouse gas emissions calculation.

We provide a detailed methodology for estimating emissions related to batteries, followed by similar methodologies for CSP, PV panels, and wind turbines. Electrolyzers' hydrogen generation is excluded from this analysis as it is assumed to be used as feedstock in the chemical sector. It is important to note that we use prospective life cycle assessment results, as carbon intensity values vary over time. Having this roadmap in mind, we turn your attention to the D.4.1 subsection which is related to batteries.

D.4.1: Battery electric vehicles

As aforementioned, we assume that batteries are primarily designed for EVs (Figure S1). Hence, we estimate the difference in greenhouse gas emission stemming from shortages in battery capacities ($ACE^{BATEV}_{n,s}$, in [ton CO_2-eq]) by assuming that the missing transportation service by electric vehicles would be replaced by an alternative mean ($ACE^{BATEV,\,Service}_{n,s}$) (Eq. S33).

$$ACE^{BATEV}_{n,s} = -ACE^{BATEV,\,IAMs}_{n,s} + \left(ACE^{BATEV,\,Opt}_{n,s} + ACE^{BATEV,\,Service}_{n,s}\right) \qquad \forall n,s \qquad \text{(S33)}$$

Here, $ACE^{BATEV,\ IAMs}_{n,s}$ and $ACE^{BATEV,\ Opt}_{n,s}$ represent the greenhouse gas emissions incurred by EVs according to the capacity estimated by IAMs and our optimization model, respectively [ton CO_2-eq]. Note that we calculate life cycle (instead of direct) emissions, thus considering also the emissions incurred while producing the energy required to feed the batteries.

In turn, the life cycle greenhouse gas emissions that would occur if we could develop the capacity of batteries projected by IAMs ($ACE^{BATEV,\ IAMs}_{n,s}$) are calculated from the energy delivered by batteries ($ED^{BATEV,\ IAMs}_{n,s}$, estimated with Eq. S26 [MJ]), the energy required by a battery EV to transport a tonne over a km in year *n* (ER^{BATEV}_{n}, in [kJ/t·km]), and the carbon intensity of a battery EV in year *n* (CI^{BATEV}, in [ton CO_2-eq/t·km_{BEV}]) (see Eq. S34).

$$ACE^{BATEV,\ IAMs}_{n,s} = ED^{BATEV,\ IAMs}_{n,s} \cdot \frac{1}{ER^{BATEV}_{n}} \cdot CI^{BEVEV}_{n} \cdot 1000 \qquad \forall n,s \tag{S34}$$

Acknowledging that EVs performance improves over time and also their carbon intensity will vary over time, we resort to prospective LCA to estimate the value of CI^{BEVEV}_{n} for different years *n* (Table S17). Prospective LCA methodology is discussed in section D.4.3

Next, we use Eq. S35 to estimate the life cycle greenhouse gas emissions for the actual capacity of batteries that could be manufactured according to the optimization model ($ACE^{BATEV,\ Opt}_{n,s}$, in [GWh]).

$$ACE^{BATEV,\ Opt}_{n,s} = ED^{BATEV,\ Opt}_{n,s} \cdot \frac{1}{ER^{BATEV}_{n}} \cdot CI^{BATEV}_{n} \cdot 1000 \qquad \forall n,s \tag{S35}$$

This equation is analogous to Eq. S34, but uses $ED^{BATEV,\ Opt}_{n,s}$ instead of $ED^{BATEV,\ IAMs}_{n,s}$. The values for CI^{BATEV}_{n} are also provided in Table S17.

Finally, Eq. S36 is used to estimate the life cycle greenhouse gas emissions incurred by replacing the service that would have been delivered by means of the "missing" battery EVs, with the corresponding replacement service (i.e., a diesel truck).

$$ACE^{BATEV,\ Service}_{n,s} = SED^{BATEV}_{n,s} \cdot \frac{1}{ER^{BATEV}_{n}} \cdot ER^{DICT}_{n} \cdot CI^{DICT}_{n} \cdot 1000 \qquad \forall n,s \tag{S36}$$

Here, $SDE^{BATEV}_{n,s}$ is the energy that will need to be substituted (in [GWh], as estimated by Eq. S30), ER^{BATEV}_{n} and ER^{DICT}_{n} denote the energy required by a battery electric vehicle and a diesel ignition combustion truck, respectively, to transport a tone over a km in year n [kJ/t·km], and CI^{DICT}_{n} is the carbon intensity of the diesel ignition combustion truck in year n [ton CO_2-eq/kJ_{diesel}] (Table S17).

Table S17: Results for the prospective life cycle assessment of the energy consumption and carbon intensity of diesel-engine trucks and battery EVs.

Term	Unit	2020	2025	2030	2035	2040	2045	2050
CI_n^{BATEV}	Kg CO_2-eq/t·km	0.132	0.101	0.081	0.068	0.059	0.052	0.046
CI_n^{DICT}	kg CO_2-eq/kJ	$7.56 \cdot 10^{-5}$	$6.98 \cdot 10^{-5}$	$6.60 \cdot 10^{-5}$	$6.78 \cdot 10^{-5}$	$6.94 \cdot 10^{-5}$	$6.98 \cdot 10^{-5}$	$6.98 \cdot 10^{-5}$
ER_n^{BATEV}	kJ/t·km	480	386	316	297	281	265	249
ER_n^{DICT}	kJ/t·km	1296	1239	1187	1142	1102	1069	1042

D.4.2: Concentrated solar power, photovoltaic panels, and wind turbines

An analogous procedure is followed to estimate the additional greenhouse gas emissions incurred by providing an alternative service to CSP, PV, and wind ($ACE^{T}_{n,s,Sc}$, in [ton CO_2-eq]).

$$ACE^{T}_{n,s,Sc} = -ACE^{T,IAMs}_{n,s} + (ACE^{T,Opt}_{n,s} + ACE^{T,Service}_{n,s,Sc}) \qquad \forall n,s\ T = \{CSP, PV, WIND\}, Sc = \{CP, N. \quad \text{(S37)}$$

In this equation, $ACE^{T,IAMs}_{n,s}$ and $ACE^{T,Opt}_{n,s}$ are the life cycle greenhouse gas emissions that would be released from these technologies according to the capacity estimated by IAMs (Eq. S38) and our optimization model (Eq. S39), respectively. Finally, $ACE^{T,Service}_{n,s,Sc}$ denotes the greenhouse gas emissions from the replacement energy (i.e., Eq. S40). The first two terms ($ACE^{T,IAMs}_{n,s}$ and $ACE^{T,Opt}_{n,s}$) are obtained with Eqs. S38-S39:

$$ACE^{T,IAMs}_{n,s} = ED^{T,IAMs}_{n,s} \cdot CI^{T}_{n} \qquad \forall n,s,T = \{CSP, PV, WIND\} \qquad \text{(S38)}$$

$$ACE^{T,Opt}_{n,s} = ED^{T,Opt}_{n,s} \cdot CI^{T}_{n} \qquad \forall n,s,T = \{CSP, PV, WIND\} \qquad \text{(S39)}$$

Here, $ED^{T,IAMs}_{n,s}$ and $ED^{T,Opt}_{n,s}$ correspond to the energy delivered by CSP, PV panels, or wind turbines according to the capacities derived from IAMs or our optimization model, respectively (see Eqs. S27 and Eq. S29). These are multiplied by the carbon intensity of the desired technology *T* for year *n* (CI^{T}_{n}, in [ton CO_2-eq/GWh]), as obtained from prospective LCA data reported in relevant studies[51–53] (see Table S18).

Table S18: Collected data for the prospective life cycle carbon intensity of CSP systems, PV panels and wind turbines.

Term	Unit	2020	2025	2030	2035	2040	2045	2050
CSP*	ton CO_2-eq/GWh	34	32	29	27	25	22	20
PV	ton CO_2-eq/GWh	80	72	64	56	55.2	54.4	53.6
Wind	ton CO_2-eq/GWh	20.1	19.95	19.8	17.8	15.9	15.9	15.9

* Data are related to a SCP system with storage option. Only two value (i.e., 20-34)were available and a linear regression is used.[54]

In this case, we assume electricity from the grid will replace the energy that CSP, PV, or wind should deliver ($SED^{T}_{n,s}$, as estimated by Eq.32). The emissions stemming from this substitution depend on the carbon intensity of the mix ($CI^{EM}_{n,Sc}$, in [ton CO_2-eq/GWh]), which, in turn, could vary differently over time depending on the evolution of the different technologies in the mix. Hence, two prospective scenarios *Sc*, Current Policy (CP) or Net Zero (NZ), are used to derive two different sets of carbon intensities over time, as discussed in section D.4.3 (Table S19).

$$ACE^{T,\,Service}_{n,s,Sc} = SED^{T}_{n,s} \cdot CI^{EM}_{n,Sc} \qquad \forall n,s\ T = \{CSP, PV, WIND\}, Sc = \{CP, NZ\} \tag{S40}$$

Ultimately, $ACE^{T,\,Service}_{n,s,Sc}$ denotes the greenhouse gas emissions released from the replacement service offered by the grid according to IAM scenario *s* and policy scenario *Sc* in year *n* [ton CO_2-eq].

D.4.3: Prospective life cycle assessment

To estimate the carbon intensity and energy requirements of battery electric vehicles and diesel ignition combustion truck, as well as the carbon intensity of grid mix, we use the data provided by prospective life cycle analysis. In contrast to traditional LCA, prospective LCA takes into account the impacts of future changes in the background system of LCA datasets. This approach considers potential shifts that could influence environmental impacts over time, ensuring that decisions are not solely reliant on present circumstances. To conduct a prospective analysis, we need to generate future life cycle inventories under different socioeconomic and environmental policy scenarios.

Our estimation begins with the data provided by IAMs, which project the potential development of the energy system, GHG sources, and mitigation technologies across various socioeconomic scenarios and climate policies. Next, we create a series of LCA databases, each corresponding to a specific year and scenario considered in the analysis. Here, we leverage the IAM data for the chosen scenarios and use the Premise v1.5.0 toolbox[55], to adapt the Ecoinvent v3.8 LCA database accordingly. Premise toolbox is an open-source Python library, operating on BrightWay2 V.0.8.7 [56], which is specifically crafted to enhance the Ecoinvent v3.8 database by integrating scenario data from IAMs related to five pivotal energy-intensive sectors: electricity generation, cement and steel production, road freight and passenger transport, and both conventional and alternative fuel supplies. This approach helps us to ensure that our LCA databases accurately reflect the evolving environmental impacts associated with different policy pathways and socioeconomic conditions over time.

Notably, our starting point involves using results from the REMIND model under Current Policy (CP) and Net Zero (NZ) narratives spanning the 2020-2050 timeframe. These narratives account for alterations in both technological aspects (e.g., vehicle weight) and policy implementations (e.g., decarbonization of the electricity matrix). Table S19 presents the results obtained for grid mix, while the results for battery electric vehicles are already presented in Table S17.

Table S19: Perspective life cycle results for carbon intensity of the grid mix electricity [kg CO_2-eq/kWh].

Scenarios	2020	2025	2030	2035	2040	2045	2050
Current Policy	0.508	0.425	0.361	0.310	0.274	0.236	0.207

Net zero	0.508	0.316	0.194	0.110	0.081	0.076	0.074

Although prospective LCA can help us to provide more accurate estimations, our calculations are still imperfect. First, it is worthnoting that these carbon intensity values are related to a typical battery, PV panel, or wind turbine, and are not available for specific types. Notably, life cycle grenhouse gas emissions from a battery EV only become lower than those from diesel-based cars after 2031. Therefore, in this case, only the extra emissions from 2032 untill 2050 are considered in our calculations (i.e., the negative difference that would be generated between 2020-2031 is neglected).

In addition, we acknowledge that a share of the energy provided by CSP, PV panels, and wind turbines during the period analysed (2020-2050) would be delivered beyond 2050 in practice (note the technology lifespan). Therefore, the carbon intensity of these technologies and that of the grid electricity used to compensate for shortages should include years beyond 2050. Unfortunately, these data are not available. Hence, in the absence of better data, we estimate the emissions for the whole life cycle of the technologies based on the carbon intensity of the year they would be installed.

D.5: Additional warming

In this step, we convert the additional greenhouse gas emissions into a temperature increase, using Eq. S41, as suggested by Hare and Meinshausen[57].

$$\Delta T^{T}_{n',Sc} = \frac{0.16ºC}{100\ GtCO_2} \cdot \sum_{n=2020}^{n'} ACE^{T}_{n,s,Sc} \qquad \forall n,s,T=\{Battery, CSP, PV, WIND\},\ Sc=\{CP, NZ\} \qquad \text{(S41)}$$

This equation establishes a temperature change of approximately 0.16°C for every 100 $GtCO_2$ cumulative fossil CO_2 emissions released until year *n'*. The additional fossil CO_2 emissions resulting from shortages in the capacity developed for each technology, denoted by $ACE^{T}_{n,s,Sc}$, are derived from Eqs. S33-S40. Hence, the term $\Delta T^{T}_{n',Sc}$ provides the temperature increase associated with the "lack" of each technology, according to CP and NZ scenarios, up to the specific year n' [°C].

E: Materials and their potential substitutes

Table S20 presents the list of materials that can be used for replacement.

Table S20: Materials and their potential substitutes[28].

Material	Replace by	Material	Replace by	Material	Replace by
Aluminium	Glass	Gold	Silver	Selenium	Silicon
	Paper		Palladium		Cerium oxide
	Plastic		Platinum		Tellurium
	Steel	Graphite	Molybdenum disulfide		Bismuth
	Manganese	Indium	Antimony		lead
	Titanium		Carbon		Sulphur dioxide
	Wood		PEDOT[e]	Silicon	Aluminium
	Vinyl		Copper		Gallium
	Copper		Silver		Germanium
Cadmium	Zinc		Graphene	Silver	Steel
	Nickel		Zinc		Tantalum

	Aluminium		Hafnium		Titanium
	Tin	Iron/steel	Aluminium		Aluminium
Cement	Fly ash		Plastic		Rhodium
	GGBFS[a]		Concrete	Tellurium	Bismuth
Cobalt	Barium		Wood		Calcium
	SF[b]		Glass		Lead
	Cerium		Paper		Phosphorus
	Iron	Lithium	Calcium		Selenium
	Lead		Magnesium		Sulphur
	Manganese		Mercury		Niobium
	Vanadium		Zinc		Tantalum
	Copper		Aluminium	Titanium	Ilmenite
	Ceramics		Sodic fluxes		Leucoxene
	Nickel		Potassic fluxes		Rutile
	Rhodium	Molybdenum	Boron		Slag
	Titanium		Chromium		Synthetic rutile
Copper	Aluminium		Niobium	Vanadium	Manganese
	Titanium		Vanadium		Molybdenum
	Steel		Tungsten		Niobium
	Plastic		Graphite		Titanium
Gallium	LC[c]		Tantalum		Tungsten
	SiMeOx[d]		Cadmium	Zinc	Aluminium
	In-Phosphide	Nickel	Titanium		Cadmium
	Helium-Neon	Platinum	Palladium		Plastic
	Silicon-Germanium	REE[f]	-		Molybdenum

[a] Ground granulated blast furnace slag.
[b] Strontium Ferrites.
[c] Liquid crystals from organic compounds.
[d] Silicon based complementary metal oxides.
[e] Poly (3,4-ethylene dioxythiophene).
[f] Substitutes are available for many applications but generally are less effective.

References

1 D. Huppmann *et al.*, "IAMC 1.5°C Scenario Explorer and Data hosted by IIASA." Integrated Assessment Modeling Consortium & International Institute for Applied Systems Analysis, 2018. doi: 10.22022/SR15/08-2018.15429.

2 B. Becker, M. Elisa Gil Bardají, J.-M. Durand, P. Clerens, and M. Noe, "Joint EASE/EERA recommendations for a EUROPEAN ENERGY STORAGE TECHNOLOGY DEVELOPMENT ROADMAP," 2017. Accessed: Nov. 15, 2023. Available: https://www.eera-set.eu/component/attachments/?task=download&id=312

3 B. Zakeri and S. Syri, "Electrical energy storage systems: A comparative life cycle cost analysis," *Renewable and Sustainable Energy Reviews*, vol. 42, pp. 569–596, 2015, doi: https://doi.org/10.1016/j.rser.2014.10.011.

4 I. Webster, " CPI Inflation Calculator." Accessed: Aug. 11, 2023. Available: https://www.in2013dollars.com/us/inflation/2010?amount=1

5 F. Rostami, Z. Kis, R. Koppelaar, L. Jiménez, and C. Pozo, "Comparative sustainability study of energy storage technologies using data envelopment analysis," *Energy Storage Mater*, vol. 48, pp. 412–438, 2022, doi: https://doi.org/10.1016/j.ensm.2022.03.026.

6 S. Wang *et al.*, "Future demand for electricity generation materials under different climate mitigation scenarios," *Joule*, vol. 7, no. 2, pp. 309–332, 2023, doi: https://doi.org/10.1016/j.joule.2023.01.001.

7 “BATTERIES EUROPE,” European Technology and Innovation Platform on Batteries, 2020. Available: https://ec.europa.eu/newsroom/ener/items/696024
8 IEA (2022), “Global EV Outlook 2022,” Paris, May 2022. Accessed: Nov. 13, 2023. Available: https://www.iea.org/reports/global-ev-outlook-2022
9 IEA (2023), “Energy Technology Perspectives 2023,” Paris, Jan. 2023. Accessed: Nov. 13, 2023. Available: https://www.iea.org/reports/energy-technology-perspectives-2023
10 IRENA, “Green Hydrogen Cost Reduction: Scaling up Electrolysers to Meet the 1.5^{0}C Climate Goal,” Abu Dhabi, 2020. Accessed: Aug. 16, 2023. Available: https://www.irena.org/-/media/Files/IRENA/Agency/Publication/2020/Dec/IRENA_Green_hydrogen_cost_2020.pdf
11 S. Schlichenmaier and T. Naegler, “May material bottlenecks hamper the global energy transition towards the 1.5 °C target?,” *Energy Reports*, vol. 8, pp. 14875–14887, 2022, doi: https://doi.org/10.1016/j.egyr.2022.11.025.
12 IEA, “Technology Roadmap Concentrating Solar Power,” Paris, 2010. Accessed: Apr. 26, 2024. Available: https://iea.blob.core.windows.net/assets/663fabad-397e-4518-802f-7f1c94bc2076/csp_roadmap.pdf
13 Energy Post, “Projected power sector battery storage capacity demand worldwide in 2030 and 2050, by scenario,” Statista, 2024, Available:https://www.statista.com/statistics/1417888/forecast-battery-storage-capacity-demand-worldwide-by-scenario/
14 P. Lusty *et al.*, *Study on future UK demand and supply of lithium, nickel, cobalt, manganese, and graphite for electric vehicle batteries*, 2022.
15 IEA (2021), “The Role of Critical Minerals in Clean Energy Transitions,” Paris, May 2021. Accessed: Aug. 22, 2023. Available: https://www.iea.org/reports/the-role-of-critical-minerals-in-clean-energy-transitions
16 IEA (2022), “World Energy Outlook 2022,” Paris, Oct. 2022. Accessed: Nov. 18, 2023. Available: https://www.iea.org/reports/world-energy-outlook-2022
17 IRENA, “FUTURE OF SOLAR PHOTOVOLTAIC Deployment, investment, technology, grid integration and socio-economic aspects (A Global Energy Transformation paper),” International Renewable Energy Agency, Abu Dhabi, Nov. 2019. Available: https://www.irena.org/-/media/Files/IRENA/Agency/Publication/2019/Nov/IRENA_Future_of_Solar_PV_2019.pdf
18 I. E. A, “The Role of Critical Minerals in Clean Energy Transition,” IEA, Paris, 2022. Available: https://www.iea.org/reports/the-role-of-critical-minerals-in-clean-energy-transitions
19 International Energy Agency, *World Energy Outlook 2017*. 2017. doi: 10.1787/weo-2017-en.
20 S. Carrara, P. Alves Dias, B. Plazzotta, C. Pavel, and P. O. of the E. Union, “Raw materials demand for wind and solar PV technologies in the transition towards a decarbonised energy system,” Luxembourg, 2020. doi: 10.2760/160859.
21 G. A. Blengini *et al.*, “Study on the EU’s list of Critical Raw Materials - Final Report,” European Commision, Brussels, 2020. doi: 10.2873/11619.
22 G. Wernet, C. Bauer, B. Steubing, J. Reinhard, E. Moreno-Ruiz, and B. Weidema, “The ecoinvent database version 3 (part I): overview and methodology,” *Int J Life Cycle Assess*, pp. 1218–1230, Sep. 2016.
23 M. C. Díaz-Ramírez, V. J. Ferreira, T. García-Armingol, A. M. López-Sabirón, and G. Ferreira, “Environmental Assessment of Electrochemical Energy Storage Device Manufacturing to Identify Drivers for Attaining Goals of Sustainable Materials 4.0,” *Sustainability*, vol. 12, no. 1, pp. 1–20, 2020, Available: https://EconPapers.repec.org/RePEc:gam:jsusta:v:12:y:2020:i:1:p:342-:d:303974
24 S. Lundberg, “Comparative LCA of Electrolyzers for Hydrogen Gas Production.” 2019, Available: https://www.diva-portal.org/smash/get/diva2:1331089/FULLTEXT01.pdf
25 D. Gielen, “CRITICAL MATERIALS FOR THE ENERGY TRANSITION,” International Renewable Energy Agency, Abu Dhabi, Nov. 2021. Available: https://www.irena.org/Technical-Papers/Critical-Materials-For-The-Energy-Transition
26 U. Das and C. Nandi, “Life cycle assessment on onshore wind farm: An evaluation of wind generators in India,” *Sustainable Energy Technologies and Assessments*, vol. 53, p. 102647, 2022, doi: https://doi.org/10.1016/j.seta.2022.102647.
27 Statista, “AgileIntel Research. (2023). Market volume of activated carbon worldwide from 2015 to 2022, with a forecast for 2023 to 2030 (in million metric tons).” Accessed: Jul. 20, 2023. Available: https://www.statista.com/statistics/963555/global-market-volume-activated-carbon/

28 “Mineral commodity summaries 2023,” Reston, VA, 2023. Accessed: Apr. 21, 2023. Available: https://pubs.usgs.gov/periodicals/mcs2023/mcs2023.pdf
29 Statista, “PlasticsEurope (PEMRG). (2022). Annual production of plastics worldwide from 1950 to 2021 (in million metric tons).,” Statista. Accessed: Jul. 20, 2023. Available: https://www.statista.com/statistics/282732/global-production-of-plastics-since-1950/
30 J. Hilburg, “Concrete production produces eight percent of the world’s carbon dioxide emissions.”, 2023. Available: https://www.archpaper.com/2019/01/concrete-production-eight-percent-co2-emissions/#:~:text=Currently%2C%20the%20world%20produces%204.4,to%20the%20Chatham%20House%20report.
31 R. Castilloux, “SPOTLIGHT ON DYSPROSIUM Revving Up for Rising Demand,” Apr. 2018. Accessed: Jul. 20, 2023. Available: https://www.adamasintel.com/wp-content/uploads/2018/04/Adamas-Intelligence-Spotlight-on-Dysprosium-April_2018.pdf
32 Statista, “Composites Manufacturing. (2023). Glass fiber capacity worldwide from 2011 to 2022 (in billion pounds).,” Statista. Accessed: Jul. 20, 2023. Available: https://www.statista.com/statistics/1177580/global-glass-fiber-capacity/
33 B. Terence, “Learn About Dysprosium.,” ThoughtCo. Accessed: Jul. 20, 2023. Available: thoughtco.com/metal-profile-dysprosium-2340187
34 Statista, “AgileIntel Research (ChemIntel360). (2023). Market volume of sodium silicate worldwide from 2015 to 2022, with a forecast for 2023 to 2030 (in million metric tons).,” Statista. Accessed: Jul. 20, 2023. Available: https://www.statista.com/statistics/1245255/sodium-silicate-market-volume-worldwide/
35 “Towards an International Year of Glass in 2022,” 2022. Accessed: Jul. 20, 2023. Available: https://www.iyog2022.org/images/files/77-economicsiyog-200925.pdf
36 Statista, “World Steel Association. (2022). World crude steel production from 2012 to 2021 (in million metric tons).,” Statista, 2023. Available: https://www.statista.com/statistics/267264/world-crude-steel-production/
37 C. Gao, Y. Xu, Y. Geng, and S. Xiao, “Uncovering terbium metabolism in China: A dynamic material flow analysis,” *Resources Policy*, vol. 79, 2022, doi: https://doi.org/10.1016/j.resourpol.2022.103017.
38 B. Terence, “Metal Profile: Iridium,” ThoughtCo. Accessed: Jul. 20, 2023. Available: thoughtco.com/metal-profile-iridium-2340138
39 UNEP, “Recycling Rates of Metals - A Status Report,” 2011. Accessed: May 04, 2024. Available: file:///C:/Users/Fatemeh%20Rostami/Downloads/metals_status_report_full_report_english.pdf
40 N. T. Nassar, G. W. Lederer, J. L. Brainard, A. J. Padilla, and J. D. Lessard, “Rock-to-Metal Ratio: A Foundational Metric for Understanding Mine Wastes,” *Environ Sci Technol*, vol. 56, no. 10, pp. 6710–6721, 2022, doi: 10.1021/acs.est.1c07875.
41 N. T. Nassar, T. E. Graedel, and E. M. Harper, “By-product metals are technologically essential but have problematic supply,” *Sci Adv*, vol. 1, no. 3, p. e1400180, 2015, doi: 10.1126/sciadv.1400180.
42 T. O.Liewellyn, “Cadmium (Materials Flow),” Bureau of Mines. Available: https://pubs.usgs.gov/usbmic/ic-9380/cadmium.pdf
43 A. S. Darling, “Iridium Platinum Alloys ,” *Johnson matthey technology review*, vol. 4, no. 1, pp. 18–26, 1960.
44 W. Sun, J. Su, G. Zhang, and Y. Hu, “Separation of sulfide lead-zinc-silver ore under low alkalinity condition,” *J Cent South Univ*, vol. 19, no. 8, pp. 2307–2315, 2012, doi: 10.1007/s11771-012-1276-y.
45 B. Torres, E. Montoya, P. Mendoza, Bedregal, M. Ubillus, and P. Olivera, “Determination of gold and silver in copper concentrates, using k0 neutron activation analysis,” Peru, 2002. Available: http://inis.iaea.org/search/search.aspx?orig_q=RN:34079944
46 IEA, “Critical Minerals Data Explorer,” Paris, Jul. 2023. Accessed: Nov. 15, 2023. Available: https://www.iea.org/data-and-statistics/data-tools/critical-minerals-data-explorer
47 N. LePan, “Visualizing the Size of Mine Tailings,” Elements. Accessed: Nov. 12, 2023. Available: https://elements.visualcapitalist.com/visualizing-the-size-of-mine-tailings/
48 M. Li, S. Rui, A. Abdulla, J. Tian, and S. Gao, “High energy capacity or high power rating: Which is the more important performance metric for battery energy storage systems at different penetrations of variable renewables?,” *The Journal of Energy Storage*, vol. 59, p. 106560, Mar. 2023, doi: 10.1016/j.est.2022.106560.

49 L. Miller and D. Keith, “Observation-based solar and wind power capacity factors and power densities,” *Environmental Research Letters*, vol. 13, p. 104008, Oct. 2018, doi: 10.1088/1748-9326/aae102.

50 NREL, “National Renewable Energy Laboratory, Innovation for Our Energy Future, Concentrating Solar Power.” Accessed: May 04, 2024. Available: https://library.cap-az.com/documents/meetings/10-17-2013/3_Combined_Solar_CSP.pdf

51 C. Li, J. M. Mogollón, A. Tukker, and B. Steubing, “Environmental Impacts of Global Offshore Wind Energy Development until 2040,” *Environ Sci Technol*, vol. 56, no. 16, pp. 11567–11577, Aug. 2022, doi: 10.1021/acs.est.2c02183.

52 B. Friedlander and C. Chronicle, “Returning solar panel production to US eases climate change,” CORNELL CHRONICLE . Accessed: Jan. 02, 2024. Available: https://news.cornell.edu/stories/2023/03/returning-solar-panel-production-us-eases-climate-change

53 R. Frischknecht *et al.*, “Life Cycle Assessment of Future Photovoltaic Electricity Production from Residential-scale Systems Operated in Europe,” Mar. 2014. Accessed: Jan. 02, 2024. Available: https://iea-pvps.org/key-topics/iea-pvps-task-12-life-cycle-assessment-of-future-photovoltaic-electricity-production-from-residential-scale-systems-operated-in-europe-2015/

54 S. Klein and E. Rubin, “Life cycle assessment of greenhouse gas emissions, water and land use for concentrated solar power plants with different energy backup systems,” *Energy Policy*, vol. 63, pp. 935–950, Dec. 2013, doi: 10.1016/j.enpol.2013.08.057.

55 R. Sacchi *et al.*, “PRospective EnvironMental Impact asSEment (premise): A streamlined approach to producing databases for prospective life cycle assessment using integrated assessment models,” *Renewable and Sustainable Energy Reviews*, vol. 160, p. 112311, 2022, doi: https://doi.org/10.1016/j.rser.2022.112311.

56 C. Mutel, “Brightway: An open source framework for Life Cycle Assessment,” *The Journal of Open Source Software*, vol. 2, Apr. 2017, doi: 10.21105/joss.00236.

57 B. Hare and M. Meinshausen, “How much warming are we committed to and how much can be avoided?,” *Clim Change*, vol. 75, no. 1–2, pp. 111–149, Mar. 2006, doi: 10.1007/S10584-005-9027-9/METRICS.